LUND UNIVERSITY

α-synuclein interactions with lipid membranes

Makasewicz, Katarzyna

2022

Link to publication

Citation for published version (APA):
Makasewicz, K. (2022). *α-synuclein interactions with lipid membranes*. Lund University.

Total number of authors:
1

General rights
Unless other specific re-use rights are stated the following general rights apply:
Copyright and moral rights for the publications made accessible in the public portal are retained by the authors and/or other copyright owners and it is a condition of accessing publications that users recognise and abide by the legal requirements associated with these rights.
• Users may download and print one copy of any publication from the public portal for the purpose of private study or research.
• You may not further distribute the material or use it for any profit-making activity or commercial gain
• You may freely distribute the URL identifying the publication in the public portal

Read more about Creative commons licenses: https://creativecommons.org/licenses/

Take down policy
If you believe that this document breaches copyright please contact us providing details, and we will remove access to the work immediately and investigate your claim.

LUND UNIVERSITY

PO Box 117
221 00 Lund
+46 46-222 00 00

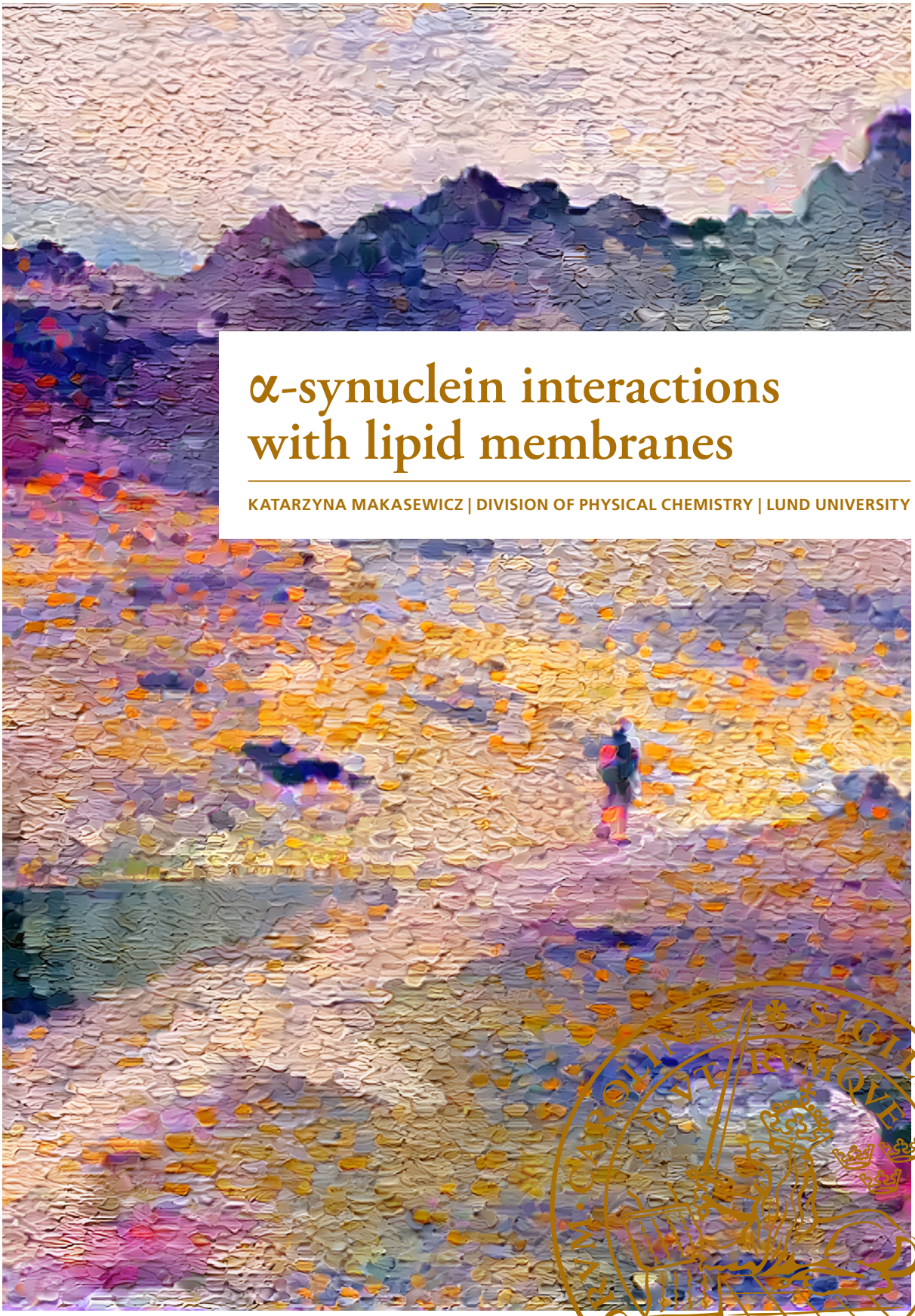

α-synuclein interactions with lipid membranes

KATARZYNA MAKASEWICZ | DIVISION OF PHYSICAL CHEMISTRY | LUND UNIVERSITY

α-synuclein interactions with lipid membranes

α-synuclein interactions with lipid membranes

by Katarzyna Makasewicz

LUND UNIVERSITY

DOCTORAL DISSERTATION

by due permission of the Faculty of Science, Lund University, Sweden.
To be defended on Friday, the 1st of April 2022 at 09:00 in Lecture hall A at the Department of Chemistry, Lund University.

Faculty opponent

Prof. Peter Kasson
Uppsala University & University of Virginia

DOKUMENTDATABLAD enl SIS 61 41 21

Organization
LUND UNIVERSITY
Department of Chemistry
Box 124
SE–221 00 LUND
Sweden

Document name
DOCTORAL DISSERTATION

Date of disputation
2022-04-01

Sponsoring organization
Funding information could go here.

Author(s)
Katarzyna Makasewicz

Title and subtitle
α-synuclein interactions with lipid membranes:

Abstract

α-synuclein is an intrinsically disordered protein implicated in synaptic vesicle trafficking at the synapse. Accumulation of α-synuclein in the form of amyloid deposits coincides with the loss of dopaminergic neurons in Parkinsons disease. These deposits, referred to as Lewy Bodies, have been shown to contain membrane lipids together with the α-synuclein amyloid fibrils and other proteins. It was also shown that lipid membranes can interfere with the process of α-synuclein amyloid formation. Thus, interactions with lipids are believed to be core to both the healthy as well as the aberrant function of α-synuclein and studies of these interactions may shed light on the mechanisms of the processes occurring both in health and in disease.

In this work, α-synuclein interactions with model lipid membranes were studied across a wide range of relative protein and lipid concentrations including excess protein and excess membrane conditions. The exchange rate between the free and membrane-bound protein was estimated to be between 20 and 100 s^{-1}. The association of the protein with membranes was characterized as strongly positively cooperative. Several different α-synuclein membrane-binding modes were identified and the factors influencing which binding mode dominates at given conditions were determined. α-synuclein-induced remodeling of lipid membranes was also studied and it was shown that protein adsorption increases the curvature of the membrane. Lipids were shown to modulate the kinetics of α-synuclein amyloid formation and to be incorporated into the formed structures.

Key words
α-synuclein, lipid membranes, peripheral membrane-binding protein, cooperativity, membrane remodeling, membrane curvature, amyloid formation, protein-lipid co-aggregation

Classification system and/or index terms (if any)

Supplementary bibliographical information

Language
English

ISSN and key title

ISBN
978-91-7422-870-0 (print)
978-91-7422-871-7 (pdf)

Recipient's notes

Number of pages
228

Price

Security classification

I, the undersigned, being the copyright owner of the abstract of the above-mentioned dissertation, hereby grant to all reference sources the permission to publish and disseminate the abstract of the above-mentioned dissertation.

Signature Katarzyna Makasewicz

Date 2022-02-21

α-synuclein interactions with lipid membranes

by Katarzyna Makasewicz

LUND UNIVERSITY

This doctoral thesis is constructed as a summary of research papers and consists of two parts. An introductory text puts the research work into context and summarizes the main conclusions of the papers. Then, the research publications themselves are reproduced. The research papers may either have been already published or are manuscripts at various stages.

Cover photo: Aritificial Intelligence image based on a photo of High Tatra Mountains, Slovakia © 2022 Katarzyna Makasewicz

© Katarzyna Makasewicz 2022

Faculty of Science, Department of Chemistry, Division of Physical Chemistry

ISBN: 978-91-7422-870-0 (print)
ISBN: 978-91-7422-871-7 (pdf)

Printed in Sweden by Media-Tryck, Lund University, Lund 2022

Media-Tryck is a Nordic Swan Ecolabel certified provider of printed material. Read more about our environmental work at www.mediatryck.lu.se

MADE IN SWEDEN

”One morning (and it will be soon), when everyone wakes up as a writer,
the age of universal deafness and incomprehension will have arrived”
Milan Kundera, ”The book of laugther and forgetting” 1978

Table of Contents

Popular scientific summary iv
List of Publications vi
Author Contributions vii
Abbreviations viii

1 Proteins, lipids and membranes 1

2 α-synuclein interactions with lipid membranes 9

2.1 α-synuclein 10
2.2 α-synuclein association with lipid membranes 11
2.3 α-synuclein membrane-binding modes 18
2.4 Dynamics of α-synuclein in the membrane-bound state . . . 24
2.5 Kinetics of α-synuclein association with membranes 26
2.6 Cooperativity of α-synuclein association with lipid membranes 34
2.7 Curvature effects versus packing defects 40
2.8 α-synuclein-induced deformation of lipid membranes 41
2.9 α-synuclein amyloid formation in presence of lipid membranes 47

Scientific Publications 63

Popular scientific summary

Proteins and lipids are the building blocks of our body. In many cases, the specific function is not carried out by a single lipid or protein molecule, but by bigger structures formed by many such molecules, which are called the supramolecular structures. An example of a supramolecular structure is a lipid membrane, formed by thousands of lipid molecules arranged in two layers. Lipid membranes enclose all cells in the body and many cellular organelles. Many proteins carry out specific functions in their monomeric state, that is without forming bigger molecular assemblies. However, there are also numerous proteins, which form large structures that carry out a multitude of functions in the cell such as shape maintenance, cell division and transport processes. The properties of proteins, lipids, the supramolecular structures that they form as well as the interactions between them form the structural and functional basis of life. Studies of protein-membrane interactions may shed light on the processes underlying the healthy functioning of the body as well as on the aberrant events taking place in disease.

In the work presented in this thesis, a neuronal protein, α-synuclein, and its interactions with model lipid membranes were studied. α-synuclein is localized in vivo at a synapse - a "junction" between two neurons, where electrical or chemical signals are passed on. The signaling substances released at a chemical synapse are packaged into lipid vesicles, which are small, closed patches of a lipid membrane. Many proteins take part in the neurotransmitter release at the synapse, and α-synuclein is one of them.

In this work, we have shown that α-synuclein remodels lipid membranes leading to the formation of membrane structures with higher curvature. We have also shown that α-synuclein association with lipid membranes is a cooperative process, which means that a protein prefers to associate with the membrane where there is already some protein bound as compared to an empty membrane. It turns out that these two phenomena, cooperative binding and membrane remodeling, go hand in hand in multiple biological processes, which involve changes in membrane shape (e.g. endocytosis and exocytosis). Our findings are consistent with the proposed function of α-synuclein in synaptic vesicle trafficking.

Exactly like the healthy processes occurring in our body involve proteins and lipids (among other players), the same is true for the dysfunctional events taking place in disease. This is the case for α-synuclein as well, which has attracted a great deal of attention in the context of its aberrant

function in neurodegenerative diseases such as Parkinson's Disease. A general capability of all proteins to form supramolecular structures in the form of fibrils, happens to be a problem in some cases. Long aggregates formed by α-synuclein are found in the pathological intraneuronal inclusions, the so-called Lewy Bodies, which are a hallmark of Parkinson's Disease. It turns out that in Lewy Bodies, the protein fibers are lumped together with fragments of lipid membranes. This motivated the studies of α-synuclein aggregation in the presence of lipid membranes. In this thesis, we have studied the effect of membranes on α-synuclein aggregation, which ranges from acceleration to inhibition with respect to what happens if the protein is incubated in the absence of membranes. We have also studied α-synuclein association with membranes in conditions, in which either acceleration or inhibition of aggregation occurs in the longer time-frame to build a more complete picture of what happens before the fibrils form.

All together, the experimental findings presented in this thesis may contribute to better understanding of mechanisms governing both the healthy and the aberrant function of α-synuclein. However, what should be born in mind by both the general as well as the scientific audience, is that the studies described in this book were carried out with a physical chemistry approach. In such an approach, the extremely complicated systems of our body are simplified to the maximum and are then studied in detail. The simplicity of such systems makes it easier to find out the mechanisms governing the behavior of the studied molecules. This would be much harder when trying to achieve the same result through studies on more complicated systems. Fortunately, the same physical principles govern the behavior of simple as well as complicated systems.

List of Publications

This thesis is based on the following publications, referred to by their Roman numerals:

I **Modulation of α-synuclein membrane interaction and aggregation by the lipid-to-protein ratio**
K. Makasewicz, O. Stenström, K. Bernfur, G. Carlström, M. Akke, S. Linse, E. Sparr
To be submitted

II **On the exchange etween free and membrane-associated α-synuclein**
K. Makasewicz, S. Wennmalm, G. Carlström, S. Linse, E. Sparr
Manuscript

III **Cooperativity of α-synuclein binding to lipid membranes**

K. Makasewicz, S. Wennmalm , B. Stenqvist, M. Fornassier, A. Andersson, P. Jönsson, S. Linse, E. Sparr
ACS Chem. Neurosci. 2021, 12, 2099-2109

IV **α-synuclein-induced deformation of small unilamellar vesicles**
K. Makasewicz, S. Wennmalm, E. Sparr, S. Linse
To be submitted

V **Structural characterization of α-synuclein-membrane interaction and the resulting aggregation using small angle scattering**
C. Galvagnion, **K. Makasewicz**, A. Barclay, F. Ravnkilde Marlet, S. Linse, A. Martel, L. Porcar, E. Sparr, F. Roosen-Runge, L. Arleth, A. K. Buell
Manuscript

VI **Lipid dynamics and phase transition within α-synuclein amyloid fibrils**
C. Galvagnion, D. Topgaard, **K. Makasewicz**, A. K. Buell, S. Linse, E. Sparr, C. M. Dobson
J. Phys. Chem. Lett. 2019, 10, 7872-7877

All papers are reproduced with permission from their respective copyright holders.

Author Contributions

Paper I
K.M. designed the study together with S.L. and E.S. K.M. performed all the experimental work apart from the mass spectrometry measurements, analyzed the data and wrote the manuscript with the input from the co-authors.

Paper II
K.M. designed the study together with S.L., S.W. and E.S. K.M. performed all experimental work, analyzed the data and wrote the manuscript with the input from the co-authors. Fluorescence correlation spectroscopy experiments were performed by S.W. and K.M.

Paper III
K.M. designed the study together with S.L., S.W., P.J. and E.S. K.M. performed all experimental work apart from the TIRF measurements, analyzed the data and wrote the manuscript with the input from the co-authors.

Paper IV
K.M. designed the study together with S.L., S.W. and E.S. K.M. performed all experimental work apart from the FCCS and iFCCS, in which K.M. prepared the samples and S.W. perfomed the experiments. K.M. analyzed the data and wrote the manuscript with the input from the co-authors.

Paper V
K.M. performed the SAXS, CD and DSC experiments with proteinase K and temperature dependent SAXS experiments, analyzed the data and took part in writing of the manuscript.

Paper VI
K.M. performed the DSC experiments, analyzed the data and took part in the writing of the manuscript.

Abbreviations

CD	circular dichroism
CP	cross polarization
cryo-TEM	cryogenic transmission electron microscopy
DSC	differential scanning calorimetry
DLS	dynamic light scattering
DLPS	1,2-dilauroyl-sn-glycero-3-phospho-L-serine
DMPS	1,2-dimyristoyl-sn-glycero-3-phospho-L-serine
DOPC	1,2-dioleoyl-sn-glycero-3-phosphocholine
DOPE	1,2-dioleoyl-sn-glycero-3-phosphoethanolamine
DOPS	1,2-dioleoyl-sn-glycero-3-phospho-L-serine
FCS	fluorescence correlation spectroscopy
FCCS	fluorescence cross-correlation spectroscopy
iFCCS	inverse fluorescence cross-correlation spectroscopy
GUV	giant unilamellar vesicle
HSQC	heteronuclear single quantum coherence
IDP	intrinsically disordered protein
INEPT	insensitive nuclei enhanced by polarization transfer
L/P	lipid-to-protein ratio
NMR	nuclear magnetic resonance
MRE	mean residue ellipticity
PFG-STE	pulsed field gradient stimulated spin echo
SAXS	small angle x-ray scattering
SANS	small angle neutron scattering
SEC	size-exclusion chromatography
SLB	supported lipid bilayer
SUV	small unilamellar vesicle
ThT	Thioflavin T
TIRF	total internal reflection fluorescence

1 Proteins, lipids and membranes

The organic molecules from which all life is built are amino acids, fatty acids, sugars and nucleotides. All of these molecules are based on the chemistry of carbon, apart from which they include smaller amounts of oxygen, nitrogen, phosphorus and sulphur. Proteins and lipids are larger molecules in which amino and fatty acids are the building blocks. In this thesis, we will deal with protein interactions with lipid membranes.

Proteins

Proteins are polymers of amino acids. A generic structure of an amino acid is shown in Figure 1.1. The core of an amino acid is an α-carbon atom connected to an amino group (-NH_2), a carboxyl group (-COOH) and a side group, which can take a variety of structures and in a simplest case is a proton. The chemical properties of the side group determine the properties of an amino acid. Depending on the side group, the amino acid can be hydrophobic, hydrophilic, positively charged, negatively charged or uncharged.

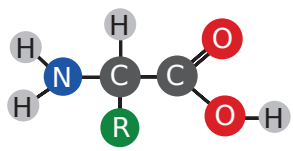

Figure 1.1 A generic structure of an amino acid. The letters H, N, C and O represent the hydorgen, nitrogen, carbon and oxygen atoms, respectively. R represents the side group, which can take many forms and in the simplest case is a hydrogen.

Proteins form through a condensation reaction where a carboxylic group of one amino acid reacts with an amino group of another amino acid, which results in the formation of a peptide bond with a water molecule being the by-product. All the proteins in biology are heteropolymers of 20 different amino acids. The sequence of the amino acid residues in a protein chain is called the primary structure. The chains of most proteins adopt some secondary structure. The two most common types of protein secondary structure are an α-helix and a β-sheet, which differ in the hydrogen bonding pattern.

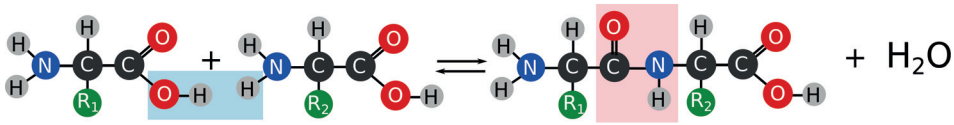

Figure 1.2 Formation of a dipeptide in a condensation reaction of two amino acids. A peptide bond (O=C-N-H) forms and a water molecule is released. The C-N bond has a partial double bond character and all four atoms involved in the peptide bond lie in the same plane. In a polypeptide chain, the available conformations are determined by the geometry of the peptide bond and steric clashes of the side groups (R).

Protein folding is a spontaneous process and the thermodynamic stability of the folded state is determined by the difference in the free energy between the folded and unfolded states. The major driving force for protein folding is the hydrophobic effect. A hydrophobic moiety is unable to participate in hydrogen bonding with water molecules and disturbs the dynamic hydrogen bonding network when introduced into an aqueous solvent. This results in water being more "structured" in the vicinity of hydrophobic molecules, which corresponds to lowered entropy. The translational freedom of water molecules, and with that the entropy, is increased when the the hydrophobic residues cluster together. Another favorable contribution to the free energy of protein folding are the enthalpic effects due to the interactions in the folded state such as hydrogen bonds, salt bridges and van der Waals forces. The decrease in the configurational entropy of the polypeptide chain opposes protein folding and lowers the free energy difference between the folded and unfolded states. The balance between the above described forces determines the structure of the folded state.

The higher levels of protein structure are the tertiary structure, which describes how the different protein segments are arranged in space, and the quaternary structure, which describes the self-assembly of more than one macromolecule. Not all proteins possess tertiary and quaternary structures.

A paradigm of high importance in molecular biology states that the unique primary structure of a protein determines its unique 3D structure, which in turn determines its also unique function. This structure-function paradigm was challenged as more and more proteins were discovered whose functionality is determined by their lack of a stable structure[1]. The so-called intrinsically disordered proteins (IDPs) do not fold into a well-defined three-dimensional structure but exist as an ensemble of dynamically inter-converting conformations. Contrary to proteins that adopt a specific fold, in the case of IDPs the state of a dynamic equilibrium

between different conformations is lower in free energy than a single or a narrow distribution of conformations[2]. The energy landscape of an IDP is relatively flat (Figure 1.3B) when compared to an energy landscape of an ordered protein (Figure 1.3A), which has a unique, stable and kinetically accessible minimum at given conditions.

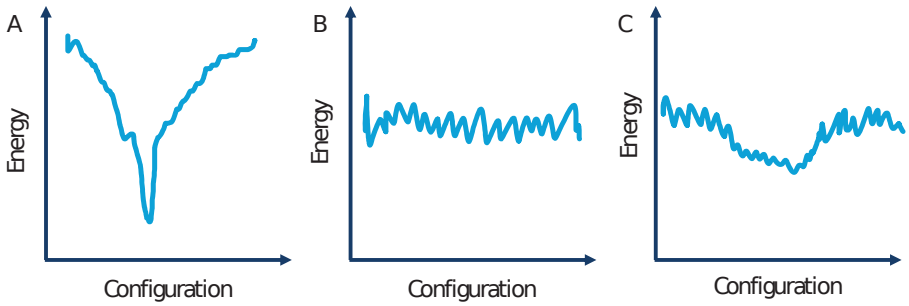

Figure 1.3 Schematic one dimensional protein folding energy landscapes. A) Funnel-like energy landscape of a protein, which adopts a unique 3D structure corresponding to a global energy minimum. B) A flat energy landscape of an intrinsically disordered protein in absence of any binding partners with many local minima and lacking a well-defined global minimum. C) Energy landscape of an intrinsically disordered protein in the presence of a binding partner e.g. α-synuclein in the presence of phospholipid membrane.

Exactly as in the case of ordered proteins, where the information dictating the structure of their native state is encoded in their amino acid sequence, the information dictating the lack of folded structure in the disordered proteins is also determined by their primary structure. The specific sequence characteristics of intrinsically disordered proteins, which enable them to be disordered and stable at the same time, include high content of charged and polar amino acids as well as low content of hydrophobic, bulky and aromatic residues.

Interestingly, IDPs do not remain disordered at all times but can adopt a well-defined secondary structure in the presence of a binding partner, in which case the energy landscape of the complex has a more or less well-defined minimum (Figure 1.3C). A protein of central interest to this work, α-synuclein, is unstructured in aqueous solution, but a large segment of its sequence is able to adopt an amphiphatic α-helix upon binding to different interfaces such as the air-water interface, micelles and lipid membranes[3-5]. The structure and properties of α-synuclein will be discussed in Chapter 2.

Phospholipids

Lipids are derivatives of fatty acids, which are hydrocarbon chains with a carboxyl group (-COOH) at the end. Lipids take on a multitude of structures and carry out a multitude of functions. In this work, we will be mainly concerned with phospholipids.
Phospholipids are a family of lipids with a glycerol backbone substituted with two fatty acids and a phosphate moiety. The phosphate group can be substituted by different compounds, the most common of which are hydrogen, glycerol, choline, serine and ethanolamine. Such substitutions result in lipid molecules called phosphatidic acid, phosphatidylglycerol, phosphatidylcholine, phosphatidylserine and phosphatidylethanolamine. Figure 1.4 shows the structures of two lipids, 1,2-dioleoyl-sn-glycero-3-phosphocholine (DOPC) and 1,2-dioleoyl-sn-glycero-3-phospho-L-serine (DOPS), employed as building blocks of model systems in the work presented in this thesis.

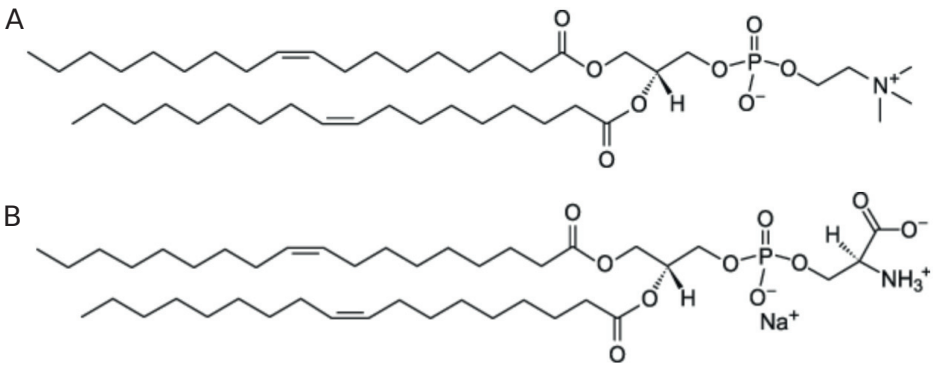

Figure 1.4 The structures of two phospholipids employed as the constituents of the model membranes used in the work presented in this thesis. A) 1,2-dioleoyl-sn-glycero-3-phosphocholine (DOPC) B) 1,2-dioleoyl-sn-glycero-3-phospho-L-serine (DOPS). Due to the unsaturation in the acyl chains, the gel-liquid crystalline transitions of membranes composed of such lipids occurs below 0°C.

The long hydrocarbon chains and the polar headgroup endows the phospholipid molecule with its most important characteristic - amphiphilicity. The fact that a phospholipid molecule is amphiphilic means that one part of it is hydrophobic (the acyl chains) and the other part is hydrophilic (the headgroup). This characteristic determines the behaviour of lipids in water, as well as in other hydrogen-bonding solvents.

Lipid membranes

The lipid bilayer is the building block of all biological membranes including the cell membrane, the cell organelles and the lipid vesicles transporting signalling substances between cells. In a lipid bilayer, the lipid molecules are arranged into two monolayers (also called leaflets) so that the hydrophobic chains of the two monolayers are in contact with each other and the hydrophilic headgroups are facing the solvent (Figure 1.5). A typical bilayer is 4-5 nm thick with the thickness depending on the length of the hydrocarbon chains of the constituent lipids. Similarly as in the case of protein folding, the most important driving force for lipid self-assembly is the hydrophobic effect.

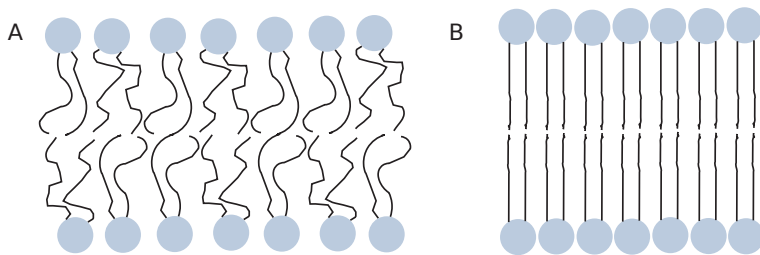

Figure 1.5 A lipid bilayer is composed of two lipid monolayers. The lipid headgroups face the solvent, while the hydrophobic chains face each other. A) A lipid bilayer in a liquid crystalline state. The hydrophobic chains are in the "melted" state, which means that they have significant conformational freedom. B) A lipid bilayer in a gel state. The hydrophobic chains are extended and have very little conformational freedom. Note that the area per headgroup in the liquid crystalline state is much greater than in the gel state. This entails that the exposure of the hydrophobic interior of the bilayer is greater in the liquid crystalline state than in the gel state.

One of the most important characteristic of biomembranes is their fluidity. In a fluid bilayer, the individual lipid molecules diffuse rapidly within the plane of the membrane with the lateral diffusion constant of around 1 $\mu m^2/s$[6]. The movement of phospholipid molecules from one leaflet to the other, the so-called "flip-flop", occurs on much longer timescales ranging from minutes to hours, as it involves the transfer of polar and/or charged moieties through the hydrophobic interior of the bilayer.
The fluidity enables biomembranes to adapt to the changes in the environment by changing the local composition, local or global curvature and topology. The lipid membranes in the gel state where the lipid molecules adopt a crystalline packing are not common in living systems[7]. Such membranes may, however, be used as model systems to investigate the role

of membrane fluidity in different processes.
A very important property of a lipid bilayer is its permeability to small uncharged molecules such as H_2O, O_2 and CO_2, and small ions such as H_3O^+ and OH^-, and impermeability to larger ions and hydrophilic molecules. The impermeability of the membrane to a given molecule may give rise to an imbalance in its concentration across the membrane (e.g. inside and outside of the vesicle or a cell). Such an osmotic imbalance may lead to the deformation of the membrane[8,9].
The lipid bilayer can be considered a two-dimensional fluid but at the same time its structure is very stable. The extremely low solubility of the bilayer-forming lipids in water ensures that membranes do not dissociate when the lipid concentration in the solution decreases. The consequence of the very low solubility of such lipids is that in the absence of changes in membrane topology (processes such as fusion and fission), the number of lipid molecules in the membrane and thus its surface area can be considered constant.
Lipids are not the only constituents of biological membranes. Such membranes contain a wide variety of proteins interacting with the bilayer in different ways. The proteins, which span the bilayer are called "integral membrane proteins" and are characterized by a very low dissociation rate. Other proteins, peripheral membrane proteins, interact with the membrane transiently and do not penetrate deeply into the acyl chain region. An example of a peripheral membrane protein is α-synuclein, whose interactions with membranes will be the focus of this thesis.

2 α-synuclein interactions with lipid membranes

2.1 α-synuclein

α-synuclein is a small neuronal protein localized *in vivo* to presynaptic termini. α-synuclein sequence consists of 140 amino acids and its characteristic feature is a polarized charge distribution. It can be subdivided into three regions of substantially different character (Figure 2.1). The N-terminal segment of the protein (residues 1-60) is rich in positively charged residues (18 charged residues in total, in which 10 lysines). A region spanning residues 61-95 is called a Non Amyloid Component (NAC) domain, which originates from the discovery of this peptide fragment in amyloid β plaques[10]. NAC domain is rich in hydrophobic residues and contains only two charged amino acids. It forms the core of α-synuclein amyloid fibrils, whose formation is associated with a range of neurodegenerative diseases. The sequence segment 1-95 contains a recurring 11-residue periodicity with the consensus sequence KTKEGV, which mediates membrane binding. The C-terminal part of α-synuclein (residues 96-140) is highly charged with a total of 15 acidic residues.

The normal function of α-synuclein is most commonly described in the literature as elusive. The protein was shown to interact with synaptic vesicles (vesicles that contain neurotransmitters as cargo and are released at the synapse) and other synaptic proteins such as synaptobrevin-2, synapsin III, VMAT2[11]. On the basis of these findings, it is hypothesized that α-synuclein is involved in synaptic plasticity, neurotransmitter release, synaptic vesicle trafficking and the maintenance of the synaptic vesicle pool[12,13].

The amyloid fibril formation of α-synuclein is associated with Parkinson's Disease among other neurodegenerative diseases. The mutations associated with Parkinson's Disease are located in the N-terminal segment of the protein (A30P, E46K, H50Q, G51D, A53E, A53T)[14].

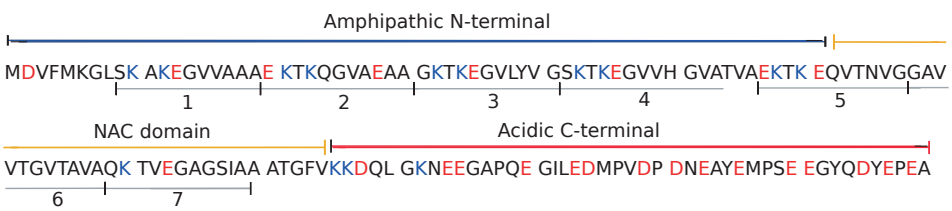

Figure 2.1 α-synuclein sequence. Acidic and basic amino acids are highlighted in red and blue, respectively. The seven 11-residue repeats of a consensus sequence KTKEGV are marked below the sequence.

2.2 α-synuclein association with lipid membranes

In this section, the structural features of α-synuclein, which determine its ability to associate with membranes will be discussed alongside the effects of membrane properties and external conditions on the interaction.
The KTKEGV periodicity in the 1-95 segment of α-synuclein enables the protein to fold into an α-helix[3]. When this part of the sequence is projected onto a helical wheel, the polar residues are localized to the opposite face of the helix than the non-polar residues (Figure 2.2). An α-helix with such arrangement of polar and non-polar residues is called amphipathic. In α-synuclein amphipathic α-helix, the polar and non-polar faces are flanked by charged residues. An amphipathic α-helix has been recognized to be an important structural motif of lipid membrane binding proteins, such as exchangeable apolipoproteins and N-BAR proteins[15-17].

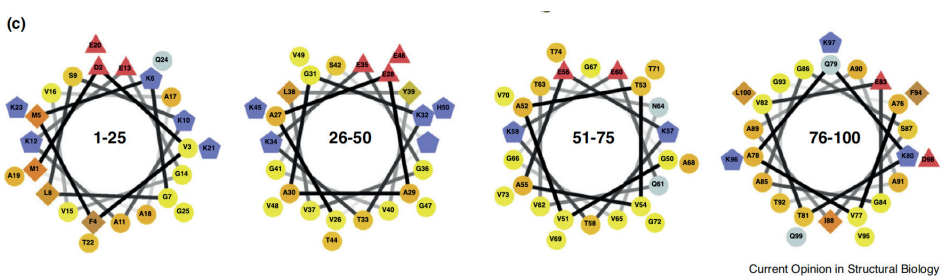

Figure 2.2 Projections of the first 100 residues of α-synuclein on a helical wheel. The hydrophobic residues are plotted in yellow, positively charged in blue, negatively charged in red. The amphipathicity, that is separation of the polar and non-polar residues to opposite faces of the helix, is strongest closest to the N-terminus and becomes progressively weaker towards C-terminus. Adapted with permission from reference[18]

Based on the presence of these specific structural motifs in α-synuclein sequence, Davidson at al[3] hypothesized that the protein should be able to associate with lipid membranes and that the association should stabilize α-helical secondary structure. The authors showed that α-synuclein indeed associates with membranes with acidic lipid content, but not with membranes composed of only zwitterionic lipids. The association is accompanied by a conformational transition from a random coil to α-helix of the (maximum) first 97 residues, with the segment 98-140 remaining in a disordered conformation. α-synuclein amphipathic helix inserts shallowly into the outer headgroup region of the bilayer[19]. The disordered C-terminus extends into the solution like a charged polymer brush. The thickness of the brush layer formed by the C-termini was estimated to be around 6 nm[20]

and was shown to decrease with increasing salt concentration[19] consistent with screening the electrostatic repulsion between the negatively charged side chains.
The first studies of the structured state of α-synuclein were done using detergent micelles as a model system. Ulmer et al[4] solved the structure of α-synuclein associated with an SDS micelle based on NMR data. The micelle-bound α-synuclein adopts a broken helix conformation with an N-terminal helix spanning residues 3-37 and C-terminal helix spanning residues 45-92 in an anti-parallel arrangement. The residues 93-97 form an extended linker and the residues 98-140 an unstructured tail. There has been much debate on whether the protein adopts a broken helix conformation or binds as a long extended helix on surfaces with lower curvature such as lipid vesicles. There are reports in favor of the broken helix[21,22], extended helix[23] and an equilibrium between these two states[24,25].

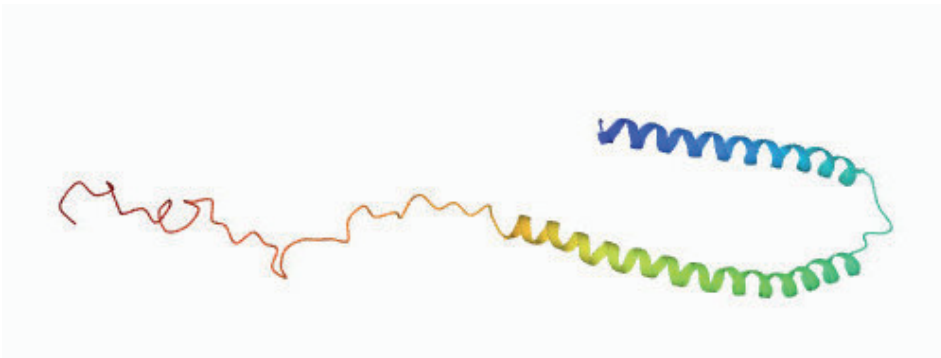

Figure 2.3 NMR structure of an SDS micelle-bound α-synuclein[4]. The protein adopts a broken helix conformation, consisting of an N-terminal helix spanning residues 3-37, a C-terminal helix spanning residues 45-92 connected with flexible linker spanning residues 38-44. The C-terminal segment rich in negatively charged residues remains disordered.
Adapted from: https://www.rcsb.org/structure/1xq8

The role of electrostatics

The fact that α-synuclein associates with negatively charged membranes (and SDS micelles) may seem peculiar given that the overall charge of the protein is negative (-7 at pH 5.5). However, the charge distribution is inhomogeneous across the α-synuclein sequence. As it was shown in Figure 2.1, the positively charged residues are most abundant in the N-terminal part of the protein (charge +4 at pH 5.5), while the negatively charged residues are much more abundant in the C-terminal segment (charge -11

at pH 5.5). The electrostatic attraction between the negatively charged lipids and the overall positively charged N-terminal part of α-synuclein are expected to bring the protein close to the charged membrane surface and facilitate the association. The electrostatic attraction between the negatively charged lipid headgroups and the positively charged side chains in the folded protein are expected to stabilize the membrane-associated state. The electrostatic repulsion between the negatively charged C-terminal segments of the protein molecules bound to the membrane in vicinity of each other as well as the repulsion between the C-terminal segments and the charged membrane surface are in turn expected to destabilize the membrane-bound state.
Davidson et al[3] showed that an increase in the ionic strength of the solution leads to a decrease in the amount of membrane-associated α-synuclein. However, the interaction could not screened completely even at high ionic strength. This result suggested that electrostatics are not the only force that plays a role in α-synuclein interactions with membranes.

The role of hydrophobic interactions

The amphipathicity of the α-helix formed by α-synuclein on the surface of a lipid membrane, suggests that hydrophobic interactions play a role in the interaction. Indeed, it has been shown that α-synuclein associates with bilayers in liquid crystalline phase, while much less association was observed in the case of gel phase bilayers[26] (the association of α-synuclein with gel phase membranes will be discussed in Section 2.7).
In a bilayer in a liquid crystalline state, the acyl chains have much more conformational freedom than in the gel state. This results in a larger average area per headgroup (as shown in a Figure 1.5), which entails a greater exposure of the hydrocarbon interior of the bilayer. The fact that α-synuclein associates to a much greater extent with fluid membranes than with gel phase membranes[26] indicates that favorable hydrophobic interactions with the exposed regions of the membrane core are vital for the association to occur. Indeed, more adsorption of α-synuclein was detected to DOPC:DOPS membranes than to POPC:POPS membranes with the same charge content and under the same solution conditions, which is ascribed to the greater area per headgroup in the DOPC:DOPS membrane as the unsaturated chains are more bulky[19,27]. It should be noted that apart from the increase in the exposure of the hydrophobic core above the melting temperature, which is a phenomenon specific to lipid bilayers,

there are also general effects that enable more objects to be packed on a fluid as opposed to a solid interface. The fluidity of a bilayer in the liquid crystalline state implies that the adsorbed proteins can diffuse rapidly in the plane of the membrane. This allows for reorganization and forming an optimal arrangement to accommodate closely packed proteins, which would not be possible on the membrane in the gel state[28].

Differential Scanning Calorimetry (DSC) thermogram of pure DMPS vesicles (Figure 2.4, for details on DSC, see Box 1) contains en endothermic peak corresponding to a phase transition from the gel to the liquid crystalline phase centered at 39°C. A DSC thermogram of DMPS vesicles with α-synuclein displays a broad peak centered around 25°C. The shift of the melting transition towards lower temperatures in the presence of α-synuclein indicates that the protein stabilizes the liquid crystalline phase of the membrane.

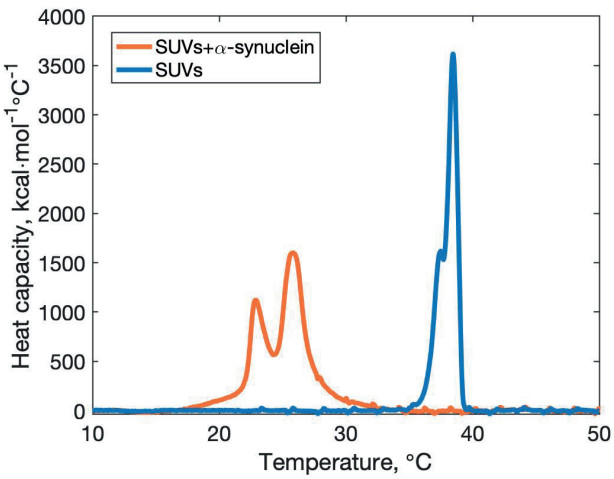

Figure 2.4 A differential scanning calorimetry thermogram of pure DMPS vesicles (blue) and DMPS vesicles with α-synuclein at L/P 30 (orange). The peaks in the thermograms correspond to the transition between gel and liquid crystalline phase of the membrane. Makasewicz et al, unpublished data.

Box 1: Differential Scanning Calorimetry
DSC is a technique with which we can study the changes in heat capacity of a sample when scanning up or down a desired temperature range. A DSC setup consists of two cells, a sample cell and a reference cell, which are placed in an adiabatic shield and are thus thermally insulated from the surroundings. Each of the cells is equipped with a heater. During a DSC scan, the temperature of both cells is either increased or decreased over a specified range, while keeping the difference in the temperature of the cells zero. When a process accompanied by a heat uptake or release occurs in the sample, the heat input to the sample cell will differ from the heat input to the reference cell. For an endothermic process (e.g. melting of a lipid bilayer) more heat will need to be supplied to the sample, while for an exothermic process, less heat will need to be supplied to the sample than to the reference cell. Therefore, the raw data in a DSC experiment is the difference of the supplied electric power between the sample and reference cells in units of energy per time. The difference in the power supplied to the sample and reference cells can be converted to the difference in heat capacity (in units of energy per degree). By integrating the area below a peak in a thermogram and normalizing it with respect to the number of moles of the material we can obtain the molar enthalpy change of the transition that occurs in the system.

Temperature dependence of α-synuclein-membrane interactions

Since hydrophobic interactions play a role in the α-synuclein association with lipid membranes, it is expected that the phenomenon displays a temperature dependence. In Paper I, we studied α-synuclein binding to SUVs using Circular Dichroism spectroscopy (CD). The CD signal at 222 nm is indicative of α-helical content of the sample (see Box 2) and increases linearly with temperature for α-synuclein in the presence of vesicles in the temperature range 5-37 °C (Figure 2.5A). We also observed a decrease in peak volume with increasing temperature in $^{15}N-^{1}H$ HSQC NMR spectra of α-synuclein and vesicles recorded in the temperature range 5-25 °C (Figure 2.5B). The decrease in peak volume implies that the number of spins contributing to the signal decreases (see Box 3). This is consistent with the expected slower reorientation rates of N-H bonds in the membrane-associated state as compared to the free protein in solution (for details on $^{15}N-^{1}H$ HSQC NMR see Box 4).
Thus, our CD and NMR data show that the amount of α-synuclein mo-

lecules associated with the membrane (provided that we start with excess of protein) increases monotonically with temperature in the studied temperature range (Figure 2.5). The strength of hydrophobic interaction is not a monotonic function of temperature, but displays a minimum around room temperature[29]. Therefore, other factors are expected to influence the observed temperature dependence. As mentioned before, the area per lipid headgroup in a membrane increases upon phase transition from the gel to liquid crystalline phase. Above the melting temperature, the area per lipid headgroup continues to increase gradually with increasing temperature[30]. This results in a slightly greater exposure of the hydrocarbon interior of the bilayer and is likely to lead to a stronger association of α-synuclein with the membrane.

It should be noted that we studied the temperature dependence of α-synuclein association with membranes in the 5-37 °C temperature range. The dependence of the interaction may in fact be a non-monotonic function of temperature over a broader temperature range. The bilayer-specific effects would then be expected to shift the minimum due to purely hydrophobic interaction.

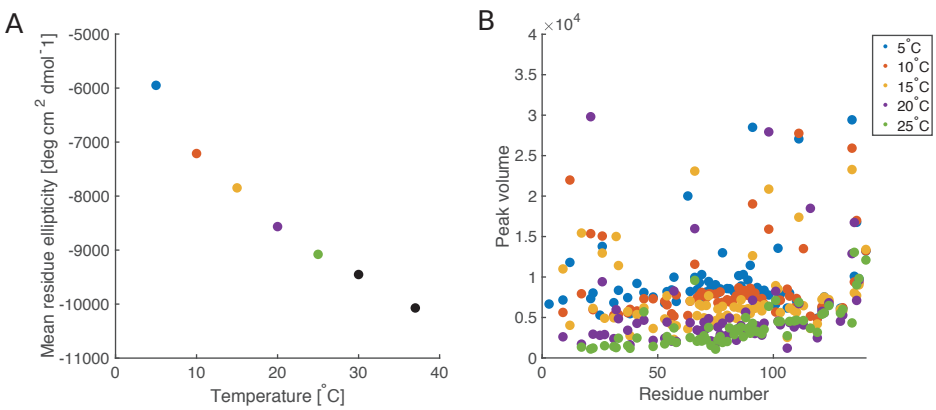

Figure 2.5 Temperature dependence of α-synuclein association with lipid membranes. A) Circular Dichroism Spectroscopy. Mean residue ellipticity at 222 nm as a function of temperature for a sample containing DOPC:DOPS 7:3 SUVs and α-synuclein at L/P 50. B) $^{15}N-^{1}H$ HSQC NMR. The volume of peaks in an HSQC spectrum of the same sample as a function of residue number in α-synuclein sequence in temperature range 5-25°C.

Box 2: Cicular Dichroism Spectroscopy in far UV

Circular dichroism spectroscopy in the far UV region (190-250 nm) is a technique commonly used to estimate the secondary structure content of a protein sample. In this wavelength range, the peptide unit is the optically active chromophore. Plane polarized light used in CD can be thought of as a sum of two circularly polarized components: right-hand and left-hand circularly polarized. The phenomenon called circular dichroism occurs when a molecule absorbs the two components to a different extent. In such a case, when the two oppositely polarized circular components are combined after passing through an optically active sample, the result is elliptically polarized light. This is why the CD spectroscopy data are often presented as ellipticity even though the measured parameter is the difference in absorption of the two circularly polarized components.

The type of the secondary structure that a protein molecule adopts (that is the arrangement of the optically active units in space and possible interactions between nearby chromophores) affects its optical activity. Macromolecules adopting α-helix, β-sheet and random coil conformations give rise to substantially different CD spectra.

The CD spectrum of an α-helix displays two distinct minima, at 208 mn and 222 nm. The CD signal at 222 nm is commonly used to track the changes in the α-helical content of the sample.

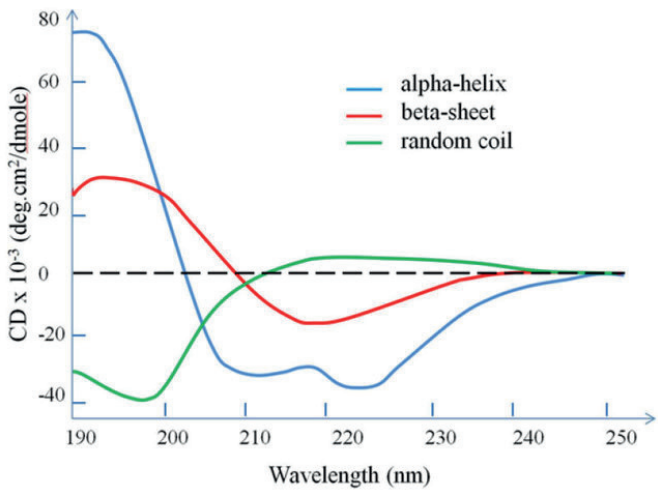

Model CD spectra of macromolecules in α-helix, β-sheet and random coil conformation. Reproduced with permission from [31].

Box 3: Peak integrals and peak volumes in NMR spectra

A typical 1D NMR spectrum is a plot of intensity as a function of frequency (see panel A below). An area under a peak in such a spectrum is proportional to the number of spins, which give rise to that peak. In a 2D NMR spectrum, each peak is plotted as a function of two frequency coordinates (see panel B below). In a 2D spectrum, the intensity dimension is going out of the plane of the paper towards the viewer, so the peaks are represented by contours similarly as mountains on a topographical map. In analogy to 1D NMR, in 2D NMR the volume of a peak is proportional to the number of spins contributing to that peak.

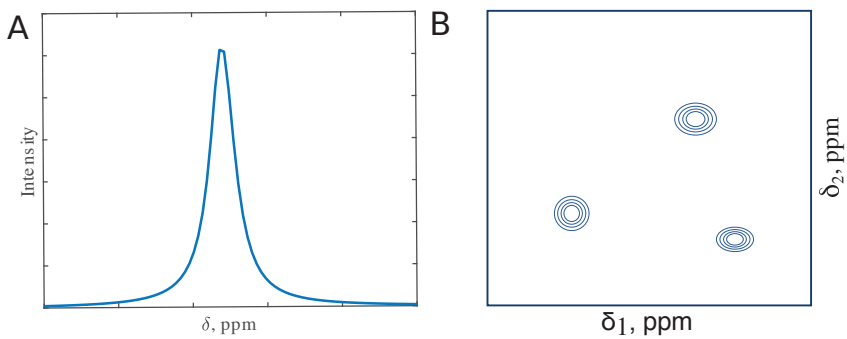

The representation of peaks in the 1D and 2D NMR spectra. A) A schematic one-dimensional NMR spectrum. The intensity is plotted as a function of chemical shift, which is the frequency difference relative to a frequency of a standard. A) A schematic two-dimensional NMR spectrum. The intensity is plotted as a function of two chemical shift coordinates. The intensity dimension is depicted as contour levels.

2.3 α-synuclein membrane-binding modes

The progressive imperfection of the amphipathicity of the α-synuclein α-helix towards the C-terminus (as illustrated on the helical wheel projection in Figure 2.2) suggests that different segments of the protein may have different affinity to the lipid membrane. Solution NMR studies revealed that α-synuclein association with membranes does not necessarily involve the full 100 residue N-terminal segment, but that there are several distinct membrane-binding modes involving sequence segments of different length (Paper I and Bodner et al[32]).

The presence of different α-synuclein-membrane binding modes was first recognized by Bodner et al[32] based on the non-uniform (with respect to the residue position in the sequence) attenuation of the peak intensities in the HSQC spectrum. The authors identified two different binding modes: one involving the sequence segment 1-20 (termed SL1) and the other involving the sequence fragment 1-100 (termed SL2). They showed that at very low L/P (L/P=1), 50 % of the protein molecules were associated with the SL1 mode. With increasing L/P, the fraction of protein molecules associated with the membrane with the binding mode involving residues 1-100 increased.
In Paper I, we studied the association of α-synuclein with small unilamellar vesicles using $^{1}\mathrm{H} -^{15}\mathrm{N}$ HSQC NMR. The HSQC spectrum of free α-synuclein contains cross-peaks corresponding to $\mathrm{N} - \mathrm{H}$ segments in all residues in the protein sequence apart from prolines (Figure 2.6, green). Upon the addition of the vesicles, the intensity of some of the peaks decreases while other peaks become unobservable (Figure 2.6, purple). The extent of these changes depends on L/P, which can be thought of as a measure of the amount of membrane surface area available for protein binding. The residues bound to the vesicle are unobservable in the HSQC spectrum. Importantly, no new or shifted resonances appear upon the addition of vesicles.

Figure 2.7 shows the attenuation of the peak volume across the α-synuclein sequence with increasing L/P ratio. The step-wise attenuation of the peak intensity implies that there are different binding modes involving sequence segments of different length. Which binding mode dominates at given conditions depends on the amount of membrane surface area available for binding and the strength of the interaction, which is modulated by changes in temperature. At 20°C and L/P 50, the first 20 residues of the α-synuclein sequence are unobservable and the remaining part of the membrane-binding segment (21-100) displays intensity attenuated by approximately 80%. The fact that the residues 1-20 are unobservable implies that all protein molecules are associated with the vesicle with this segment, which is consistent with the SL1 binding mode identified by Bodner et al[32]. The decrease in the intensity of the peaks corresponding to the segment 21-100 indicates that 80% of the protein molecules are also associated with the vesicle with this segment. This is consistent with the SL2 binding mode proposed by Bodner et al[32]. At L/P 100, the signals from the first 55 residues are unobservable, while the intensities of the 56-100 segment are attenuated by approximately 90%. This indicates that all protein molecules are associated with the vesicle with the 1-55 segment, while 90% of the protein molecules

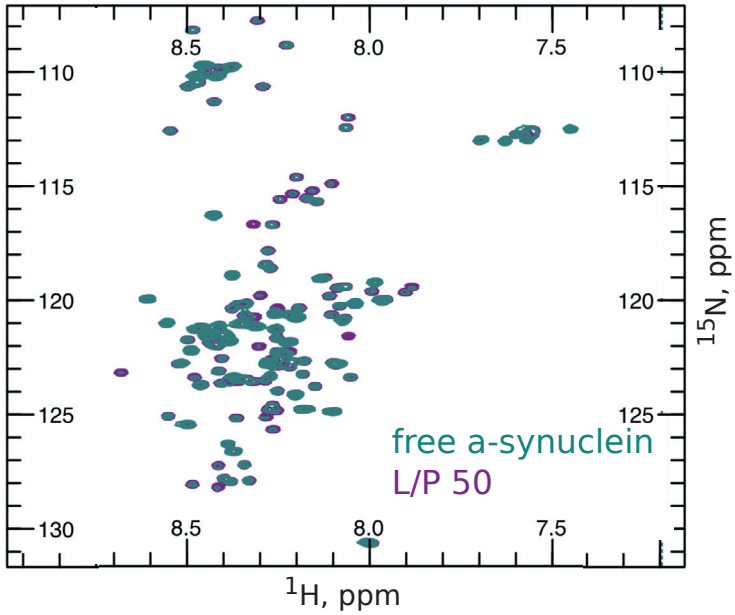

Figure 2.6 ^{1}H $-^{15}$ N HSQC spectra of free α-synuclein (magenta) and α-synuclein with DOPC:DOPS 7:3 small unilamellar vesicles at L/P 50 (purple).

are also associated with the vesicle with the 56-100 segment. At L/P 200 and 250, only the peaks corresponding to residues 100-140 are observable, meaning that all protein molecules are associated with the vesicle with the 1-99 segment. The different binding modes implied from the NMR data are depicted in cartoon in Figure 2.8.

Figure 2.7B shows the normalized peak volumes at 37°C for L/P 10, 20, 40 and 50. Interestingly, the attenuation of the peak intensity follows the same pattern as observed at 20°C, even though the changes occur in a different L/P range. The attenuation of the signal intensity at L/P 50 at 20°C is identical with the attenuation pattern at L/P 10 at 37°C. The same holds for L/P 100 at 20°C and L/P 20 at 37°C, L/P 200 at 20°C and L/P 40 at 37°C. The fact that at 37°C, stronger attenuation of the signal intensities is observed at lower membrane content is consistent with the temperature dependence of α-synuclein association with membranes discussed in Section 2.2.

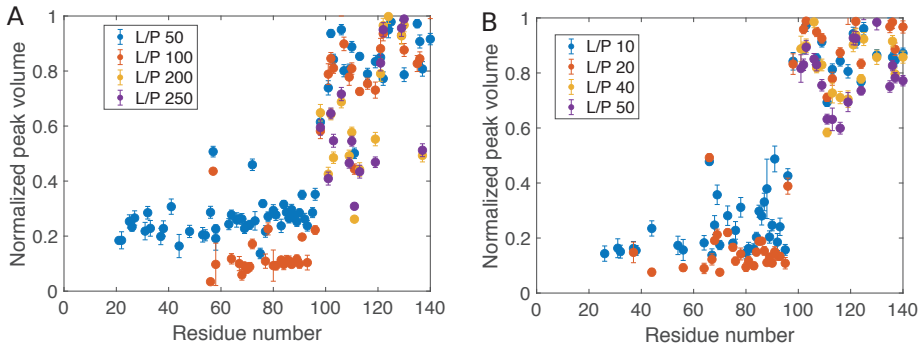

Figure 2.7 Studying α-synuclein association with DOPC:DOPS 7:3 small unilamellar vesicles (SUVs) with $^{1}\mathrm{H}-^{15}\mathrm{N}$ HSQC NMR spectroscopy. The peak volumes in the HSQC spectrum containing α-synuclein and SUVs at different L/P ratios are normalized with respect to the peak volume in the free α-synuclein spectrum and are plotted as a function of the residue number in the protein sequence. A) Normalized peak volumes for L/P 50, 100, 200 and 250 at 20°C. B) Normalized peak volumes for L/P 10, 20, 40 and 50 at 37°C.

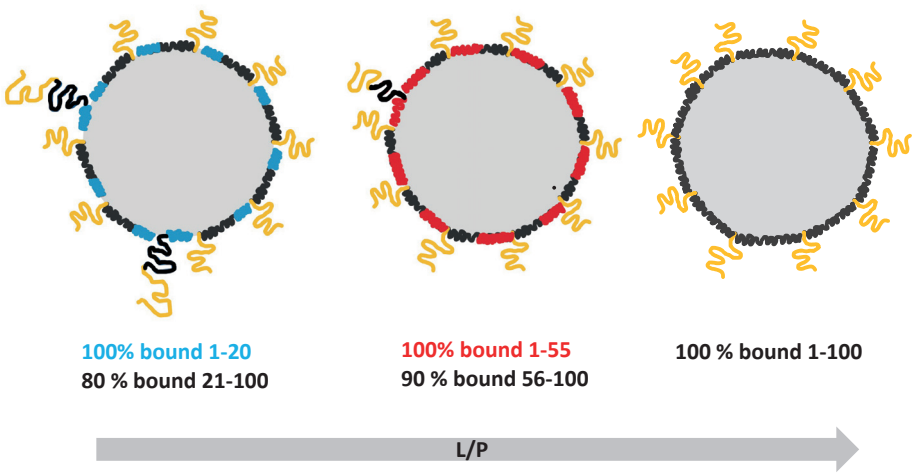

Figure 2.8 A model of α-synuclein association with lipid membranes across a broad L/P range based on $^{1}\mathrm{H}-^{15}\mathrm{N}$ HSQC NMR data. At lowest L/P considered here, which corresponds to L/P 50 in Figure 2.7A, 100% of the protein molecules are bound with the 1-20 segment, while 80% protein molecules are also bound with the 21-100 segment. At intermediate L/P, corresponding to L/P 100 in Figure 2.7A, 100% of protein molecules are bound with the 1-55 segment, while 90% of the proteins are bound also with the 56-100 segment. At high L/P, corresponding to L/P 200 and 250 in Figure 2.7A, all protein molecules are bound to the vesicle with the 1-100 segment, while the segment 100-140 remains disordered.

Perspective

The existence of different α-synuclein binding modes prompts to revisiting the current view on the analysis of the experimental data, which often relies on an assumption that the protein can occupy either of only two states: membrane-bound or free, as e.g. in determination of the equilibrium dissociation constant, K_d, in α-synuclein-membrane systems based on the changes in CD signal. Taking into account that α-synuclein associates with membranes with sequence segments of different length, the total α-helical CD signal may be due to a smaller number of long α-helices or larger number of shorter α-helices. Thus, the changes in the CD signal upon titration of α-synuclein with lipid membranes cannot be used to extract the fractions of free and bound protein and therefore not to determine the K_d. Another implication of the findings described in this section is in the context of α-synuclein amyloid formation in the presence of membranes. The fact that α-synuclein associates with membranes with fragments of different length at different L/P conditions, implies that the properties of the protein-covered membrane surface also depend on the L/P (other parameters assumed constant). This is expected to modulate the interaction of a free monomer with the membrane surface. This aspect will be further discussed in Section 2.9 devoted to α-synuclein amyloid formation in the presence of lipid membranes.

Box 4: $^{1}H-^{15}N$ HSQC NMR experiment as a protein's fingerprint

$^{1}H-^{15}N$ Heteronuclear Single Quantum Coherence is an example of a 2D NMR experiment in which one-bond correlations between a ^{15}N and a ^{1}H nuclei are detected. In an $^{1}H-^{15}N$ HSQC spectrum, as in the schematic shown in the figure below, each peak is plotted as a function of two frequency coordinates. A x,y ppm position of a peak indicates that this peak is due to a proton with a chemical shift of x ppm that is covalently bonded to a nitrogen with a chemical shift of y ppm. Since the $N-H$ bond is repeated in each amino acid unit (apart from prolines) throughout the peptide chain, each residue in the protein sequence may give rise to a peak in an $^{1}H-^{15}N$ HSQC spectrum with unique chemical shift due to the unique chemical environment. The side chains containing an NH_2 group will also give rise to peaks in a $^{1}H-^{15}N$ HSQC spectrum (each NH_2 group gives rise to two peaks at the same ^{15}N chemical shift but with two different ^{1}H chemical shifts). Changes in the chemical shifts report on the changes in the chemical environment of a given residue. This allows us to determine which residues/sequence segments take part in ligand binding. It may also happen that in the presence of a binding partner, a given peak disappears from the HSQC spectrum. This may be due to a decrease in the reorientation rate of the $N-H$ bond upon complex formation or binding to a slowly tumbling entity and subsequent line broadening. Thus, both chemical shift changes and disappearance of the peaks in an $^{1}H-^{15}N$ HSQC spectrum may provide structural information about an interaction.

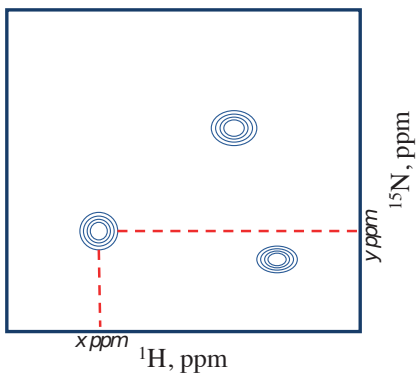

A schematic $^{1}H-^{15}N$ HSQC spectrum. A peak with frequency coordinates x and y ppm, corresponds to a proton with chemical shift of x ppm covalently bonded with a nitrogen with a chemical shift of y ppm.

2.4 Dynamics of α-synuclein in the membrane-bound state

A detailed study on the dynamics of the different segments in a membrane-associated α-synuclein was carried out by Fusco et al[33]. The authors used a combination of solid and solution state NMR experiments to show that the different segments of the membrane-bound α-synuclein possess distinctly different dynamic properties.

Box 5: Polarization Transfer NMR

Polarization transfer is a way to enhance the signals in NMR. In a Cross Polarization (CP) experiment, the polarization is transferred from one nucleus to another (e.g. from ^{1}H to ^{13}C) via dipolar couplings (through-space), which are averaged to zero by fast isotropic reorientation. In an Insensitive Nuclei Enhanced by Polarization Transfer (INEPT) experiment, the polarization is transferred from one nucleus to another through covalent bonds, which is not averaged out by isotropic reorientation. In solid samples, the signal decays very fast due to high transverse relaxation rate. Therefore, even though scalar couplings are also present in rigid molecules, the signal enhancement via INEPT will not be efficient. As a result, the CP enhances efficiently signal for segments of low molecular mobility, while INEPT enhances efficiently signals for highly mobile molecular segments. "Mobile" and "rigid" depend on the correlation time, τ_C, and order parameter, $|S_{CH}|$, of a given bond vector (e.g. $C-H$). High τ_C implies low reorientation rate, while high $|S_{CH}|$ implies anisotropic reorientation. In an INEPT spectrum, the signals of high intensity are due to bond vectors with $\tau_C < 0.01\mu s$ and $|S_{CH}| < 0.05$. In a CP spectrum, the signals of high intensity are due to bond vectors with $\tau_C > 10\mu s$ and $|S_{CH}| > 0.5$. For more detailed discussion on the subject the reader is referred to Nowacka et al[34].

The α-synuclein segment spanning residues 6-25 was implied to be very rigid when associated with the membrane as it was detected in a cross polarization (CP) experiment. The 97-140 segment was detected in an Insensitive Nuclei Enhanced by Polarization Transfer (INEPT) experiment implying high dynamics (for more information on how the combination of CP and INEPT experiments can be used to study the site-specific dynamics of molecules, see Box 5). The 26-97 residue segment was inferred to have intermediate dynamics as it was not possible to detect it in neither CP nor INEPT, implying that the segment is too mobile to be detected in a CP experiment but at the same time too rigid to be detected in an INEPT experiment. The differences in the dynamics of the different segments of

membrane-bound α-synuclein are depicted in a cartoon in Figure 2.9.

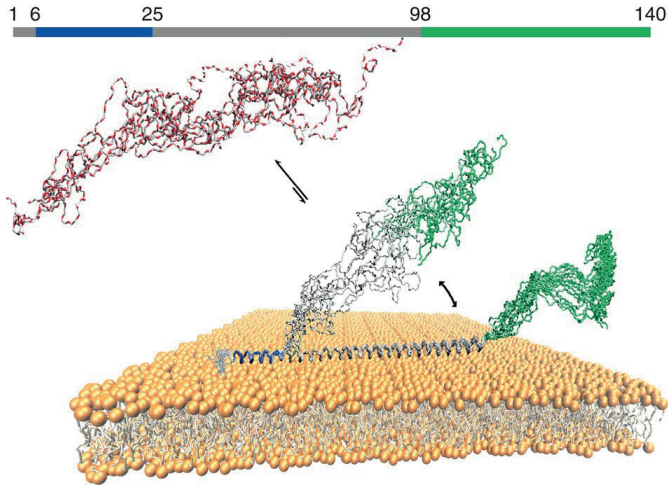

Figure 2.9 Cartoon illustrating the dynamics of different segments of membrane-bound α-synuclein. The segment spanning residues 6-25 (blue) is rigid when bound to the membrane. The C-terminal region (green) remains unstructured and highly mobile in a membrane-bound protein, while the central region (grey) displays dynamics intermediate between the rigid N-terminal part and highly dynamic C-terminal part. The conclusions on the dynamics of the different regions were drawn based on a combination of solution and solid state NMR experiments. It should be noted that only one α-synuclein molecule interacting with the membrane is depicted for clarity. In reality, more α-synuclein molecules would be bound nearby. Also, in the conditions of excess membrane (as illustrated in the cartoon) the protein would be associated with the membrane with 1-100 segment (as discussed in Section 2.3). Adapted with permission from[33].

Interactions of the C-terminal segment with the membrane

Fusco et al also employed paramagnetic resonance enhancement NMR to gain information on any transient interactions of the C-terminal segment of a bound α-synuclein molecule with the membrane[33]. The authors employed a model bilayer, which contained lipid molecules with unpaired electrons located on the headgroup. The interaction of a spin with the paramagnetic centre is a relaxation mechanism and thus the broadening of the protein resonances provides information on the proximity of different protein segments to the bilayer. Apart from detecting the broadening of resonances of the residues in the membrane-binding region, the broadening of the resonances was also detected for some of the C-terminal residues (K97, Q99, L100, A107, I112, V118). This implies that the C-terminal residues are at least transiently located in the proximity of the membrane.

2.5 Kinetics of α-synuclein association with membranes

In order to gain a more thorough picture of α-synuclein association with lipid membranes, the characterization of the dynamics of the interaction is necessary. In this section, we will first discuss the experiments designed to visualize the exchange between free and vesicle-bound α-synuclein and study the redistribution of α-synuclein between vesicles. Then, the experiments designed to estimate the timescale of the association and the timescale of the exchange between the free and membrane-bound protein will be discussed.

Visualizing the exchange between free and GUV-bound α-synuclein

In Paper II, we employed confocal microscopy to visualize the exchange between free and vesicle-associated α-synuclein employing giant unilamellar vesicles (GUVs) as a model system. Unlabelled GUVs were saturated with red-labelled α-synuclein and imaged. Then, green-labelled α-synuclein was added. Figure 2.10 shows the respective confocal images. Straight after the addition of the green-labelled protein, the GUVs appear both in the red and green channels. Thus, the exchange process is implied to have occurred in the dead-time of the experiment, that is within a couple of minutes.

Redistribution of α-synuclein between SUVs

We employed fluorescence cross-correlation spectroscopy to determine how fast α-synuclein redistributes between SUVs (Paper II). In this experiment, SUVs were first saturated with blue-labelled α-synuclein (L/P 200). At that stage, the FCCS intensity trace, shown in Figure 2.11B, contains only blue intensity spikes, which are due to SUVs decorated with blue protein passing by the focal volume (more on FCS in Box 8). In the second step of the experiment, SUVs saturated with red-labelled α-synuclein (L/P 200) were added and mixed. The emergence of overlapping blue and red spikes in the intensity trace straight after the addition of SUVs with red-α-synuclein implies that some of the proteins have exchanged between vesicles during mixing (within several seconds) (Figure 2.11C).

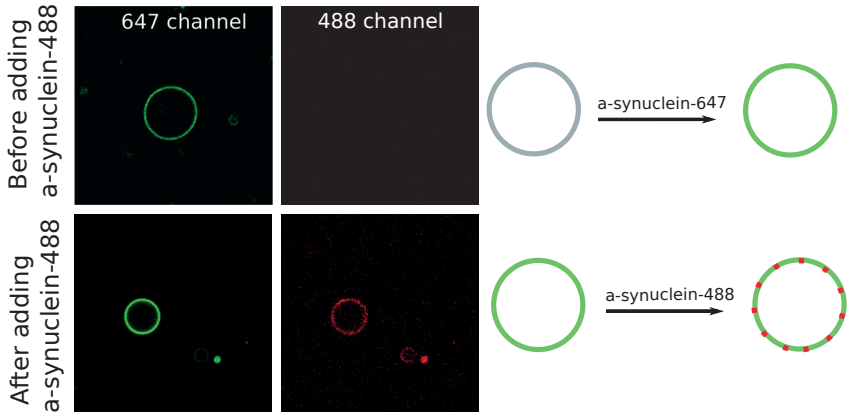

Figure 2.10 Studying the exchange between free and membrane-associated α-synuclein using confocal microscopy. Left: Confocal images of GUVs saturated with green-labelled α-synuclein (top) and after the addition of red-labelled α-synuclein (bottom). Right: Cartoons illustrating the two experimental steps.

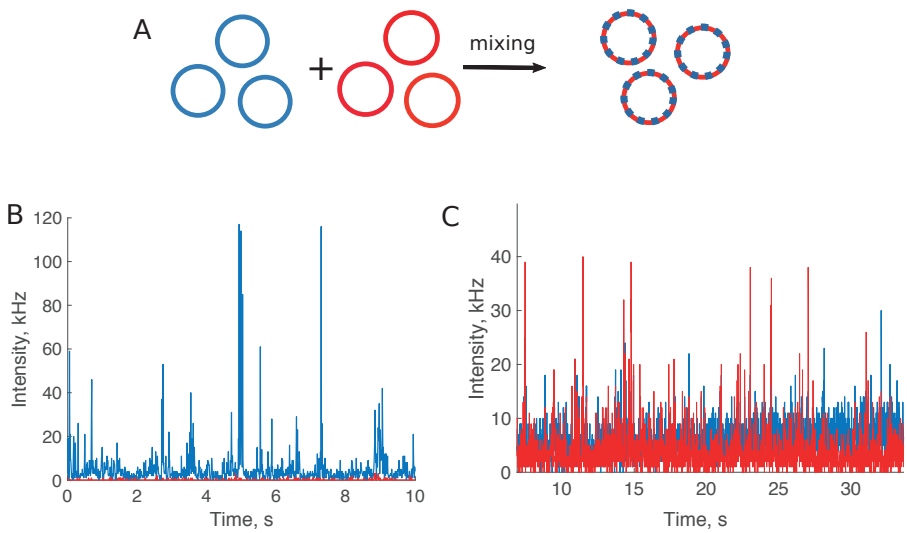

Figure 2.11 Studying the redistribution α-synuclein between SUVs using fluorescence cross-correlation spectroscopy. A) A cartoon representing the experimental steps. SUVs saturated with red-labelled α-synuclein were added to SUVs saturated with blue α-synuclein and mixed. B) The FCCS intensity trace of SUVs saturated with blue α-synuclein before the addition of SUVs saturated with red α-synuclein. C) The FCCS intensity trace after the addition of red α-synuclein and mixing. Mixing was finished at time 0 s in the intensity trace and the overlapping red and blue spikes are present immediately after.

Stopped flow SAXS study of α-synuclein association with lipid vesicles

In paper V, α-synuclein association with DMPS SUVs was studied using stopped-flow SAXS. The protein solution was injected into a DMPS vesicle dispersion and the scattering curve was acquired at several ms intervals after mixing.[i] The observed change in the SAXS curve, indicative of protein adsorption (see Box 6), occurred in the dead time of the experiment, that is within 4 ms. No further changes in the scattering pattern were observed (Figure 2.12).

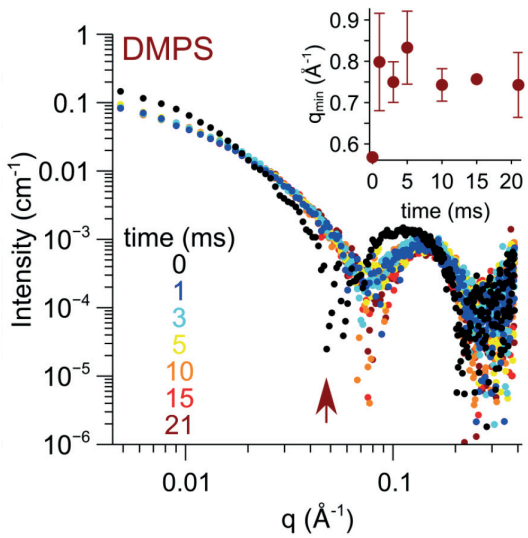

Figure 2.12 Probing the timescale of α-synuclein association with lipid vesicles using stopped-flow SAXS. The scattering pattern of pure vesicle dispersion is shown in black. The scattering patterns after the injection of α-synuclein were measured at several ms intervals. The inset shows the position of the first visible minimum in the scattering pattern indicated with an arrow. Already the first acquired pattern post mixing was characteristic of a vesicle with α-synuclein bound, and no further changes were observed with time. Thus, the association occurred during the dead-time of the experiment which was 4 ms.

[i] 20 mM phosphate buffer pH 6.5 30 °C

Box 6: Small angle x-ray scattering

When an X-ray beam impinges on a sample, some of the radiation passes through unaffected, some gets absorbed and some gets scattered. In X-ray scattering, the incident radiation is scattered as a result of interaction with electrons of the atoms in the sample. In a static scattering experiment, which provides information about the size and shape of objects in the sample, the intensity of the scattered radiation is usually measured over a range of angles. The electromagnetic waves scattered from different objects in the sample interfere constructively or destructively which gives rise to an angle dependence of the scattering intensity. The main feature of a SAXS scattering curve from a vesicle dispersion is a bilayer form factor (the bump seen in the Figure below), which reports on the electron density distribution across the bilayer: inner headgroups with high electron density, acyl chain region with lower electron density and outer headgroups with high electron density.

Protein adsorption to a vesicle results in a change of electron density distribution in the bilayer and thus in a change in the scattering curve (yellow data points in Figure below). Thus, SAXS can be employed to study protein adsorption to membranes.

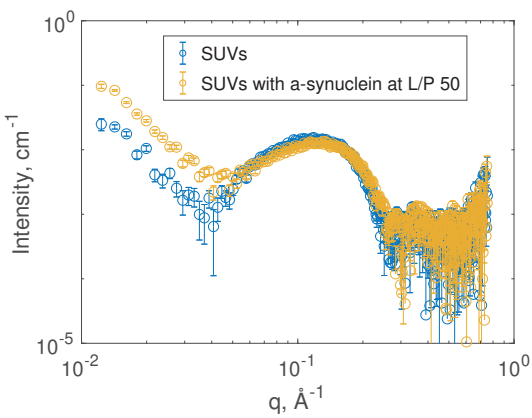

Small angle x-ray scattering curves of a pure DOPC:DOPS 7:3 SUV dispersion (blue) and of a sample containing SUVs and α-synuclein at L/P 50 (yellow). The change in the bilayer form factor upon the adsorption of the protein is due to the change in the electron density profile of the bilayer, while the increase in the intensity at low q is due to the overall higher electron density of the sample. Makasewicz et al, unpublished data.

Determination of the k_{ex}

The experimental data presented above suggest that association of α-synuclein with lipid vesicles as well as the exchange between the free and membrane-associated protein are fast relative to the timescales accessible in the confocal, FCCS and stopped-flow SAXS experiments. In the following subsections, the determination of the exchange rate between free and membrane-bound α-synuclein using NMR will be discussed.

The exchange on the NMR chemical shift timescale

In Section 2.3, the $^{1}H-^{15}N$ HSQC spectra of free α-synuclein and α-synuclein in presence of SUVs were discussed. It was mentioned that the peaks corresponding to the segments of the protein that are associated with the vesicle are invisible in the spectrum, while the remaining ones have the chemical shifts equal to those in the free protein spectrum. This together with the fact that the linewidths of the peaks that remain visible in the presence of the vesicles are not substantially broadened (see SI of the Paper I) implies that the exchange between free and membrane-bound α-synuclein is slow on the NMR chemical shift timescale. This is consistent with conclusions made by Bodner et al[32].
Whether an exchange process is slow or fast on the NMR chemical shift timescale is determined by the value of the exchange rate between the two states (in our case, free and vesicle-bound α-synuclein) relative to the difference between the frequencies of the two corresponding resonances. If $k_{ex} << \Delta$, where Δ is the frequency separation in Hz, then the exchange is slow on the NMR chemical shift timescale[35]. The above relation can be employed to estimate the timescale of the exchange process on the real-life timescale, once the chemical shifts of both states are known. Even though the membrane-bound state is invisible in the $^{1}H-^{15}N$ HSQC spectrum, we can use the theoretical chemical shifts of the given residues in an α-helix to calculate the frequency separation. The average difference between the random coil chemical shifts observed in the free α-synuclein spectrum and the theoretical values in an α-helix for the residues in the membrane-binding segment of α-synuclein is around 100 Hz. Thus, $k_{ex} << 100s^{-1}$. This should be treated as a rough estimate as the chemical shifts of residues in an α-helix interacting with a lipid membrane are expected to differ from the theoretical chemical shifts of α-helical residues.

Studying equilibrium dynamics with diffusion NMR

Another approach to estimate the value of the exchange rate between free and membrane-bound α-synuclein is to employ pulsed field gradient stimulated echo (PFG STE) NMR experiment. In this experiment, the translational diffusion of the sample components is measured in a well-defined time using gradient pulses (see Box 7). In the case of a molecule, which can occupy two states characterized by different diffusion coefficients, the possibility of detecting both states in the PFG STE experiment depends on the timescale of the exchange between them relative to the diffusion time, Δ, in the pulse sequence. Δ is the time between the onset of the consecutive gradient pulses, during which the signal is detected. If the lifetime of the two states (free protein and membrane-bound protein in our case) is much shorter than Δ (implying fast exchange), then the individual states will not be resolved. The observed decay of the signal intensity will be a single exponential with a decay constant being the population averaged diffusion coefficient. If the lifetime of the two states is longer than Δ (implying slow exchange), the observed signal decay will be a sum of exponentials, each with a characteristic diffusion coefficient.
In Paper II, we have carried out the PFG STE experiments on samples containing α-synuclein and SUVs at different L/P ratios (50, 100 and 200) to estimate the exchange rate and determine whether there are any detectable differences between the dynamics at different L/P conditions.
Figure 2.13A shows the decay of the intensity of the peaks from free vesicles, free α-synuclein, α-synuclein in presence of vesicles at L/P 100 and a MES (buffer) molecule. The peak intensities at each value of the gradient strength are normalized with respect to the peak intensity in the absence of the gradient and plotted as a function of a parameter b, which is proportional to the square of the gradient pulse strength (for details see Figure caption and Paper II). We observed the fastest decay for MES, followed by free α-synuclein, α-synuclein with SUVs at L/P 100 and free SUVs. The signal attenuation is proportional to the distance that the given molecule/particle diffused in between the gradient pulses and thus the faster the diffusion, the lower the gradient strength at which the signal will be attenuated completely. The mono-exponential character of the decay of the signal from α-synuclein in the presence of lipid vesicles implies that the lifetimes of the bound and free states are much shorter than the diffusion time, Δ, which was set to 50 ms. Thus, the rate of the exchange between the free and membrane-bound α-synuclein, k_{ex} is greater than $20s^{-1}$ ($\frac{1}{50ms}$).

In order to determine whether there any any detectable differences in dynamics at different L/P conditions, we have carried out the PFG STE experiments also for samples containing α-synuclein and SUVs at L/P 50 and 200. The intensity decay from the protein peaks in samples at all L/P ratios investigated as well as for the free protein are plotted in Figure 2.13B. With increasing L/P, the observed signal decay is slower as more protein is associated with the slowly diffusing vesicle. At L/P 200, the decay curves of the lipid and α-synuclein peaks overlap, as virtually all protein is expected to be associated with the vesicle (Figure 5C in Paper II). The monoexponential character of the signal intensity decay for α-synuclein peaks at all L/P conditions implies that, in all cases the exchange rate $k_{ex} > 20s^{-1}$.

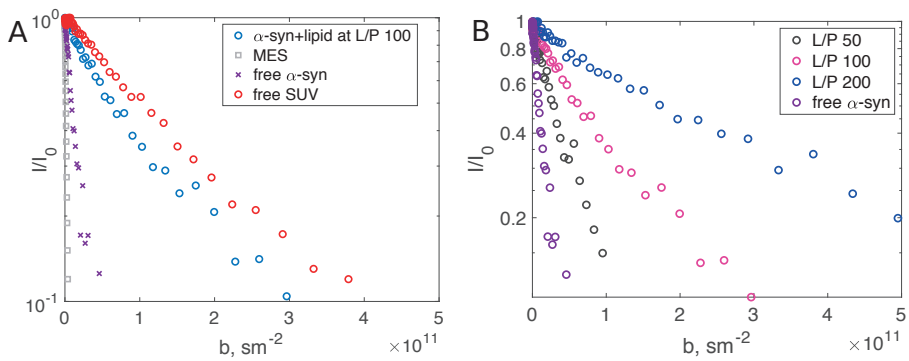

Figure 2.13 Probing the exchange rate between the free and vesicle-associated α-synuclein with pulsed-field gradient stimulated echo NMR experiment. A, B) Signal decay of different peaks as a function of a parameter b, where $b=(\gamma G\delta)^2(\Delta - \delta/3)$, where γ is the proton gyromagnetic ratio (rad/s/T), G is the gradient strength (T/m), δ is the gradient pulse length and Δ is the total diffusion time (s). Peak intensities at each value of the gradient pulse strength were normalized with respect to peak intensities in the absence of the gradient pulse. The mono-exponential decay of the peak intensity corresponding to α-synuclein in the presence of SUVs implies that the lifetimes of the free and bound states are short relative to the diffusion time (50 ms). Thus, $k_{ex} > 20s^{-1}$.

Box 7: Pulsed field gradient spin echo NMR experiment
Pulsed field gradient stimulated echo (PFG STE) NMR experiment allows to measure diffusion of the sample components. In the PFG STE pulse sequence, there is a spin echo element and gradient pulses applied with a delay time in between. The function of the gradient pulses is to dephase the magnetization of the spins that diffused along the direction of the gradient field during the so-called diffusion time, Δ. The gradient pulses have no net effect on the spins, which did not move. The dephasing of the magnetization of the moving spins results in a lowered intensity of the detected signal. The degree of the dephasing due to the gradient pulses is proportional to the gradient amplitude and to the displacement of the spin in the direction of the gradient in the diffusion time Δ. By repeating the pulse sequence at different gradient amplitudes and observing signal decay, we can determine the diffusion coefficient of the sample components.

Perspective

By combining the results of our HSQC and PFG STE NMR data, the k_{ex} at the conditions of our experiments (DOPC:DOPS 7:3 lipid system, 10 mM MES buffer pH 5.5) can be estimated to be greater than $20s^{-1}$ and less than $100s^{-1}$. This result can be compared with the values previously reported in the literature. Shvadchak et al[27] measured the kinetics of α-synuclein association with lipid vesicles using stopped-flow fluorescence. The authors employed an α-synuclein cysteine mutant (A18C) labelled with an excited state intramolecular proton transfer probe, which displays different spectral characteristics in the aqueous solvent and in a hydrophobic environment such as the interior of the lipid membrane. The changes in fluorescence intensity upon addition of α-synuclein to a DPPG vesicle dispersion were monitored in 0.02-1 ms intervals with a 2 ms deadtime. The fitting of the intensity traces with a single exponential allowed the authors to estimate the apparent exchange rate $k_{ex} = 53s^{-1}$.[ii] The authors also measured the k_{ex} of α-synuclein association with DOPC/DOPG SUVs with different relative proportions of the zwitterionic and charged lipids (mol/mol ratios 3:1, 1:1 and 1:3). They found that k_{ex} increased with increasing fraction of the charged lipids, which corresponds to a decrease in the lifetime of the membrane-bound state. The estimated k_{ex} values were 150, 330 and

[ii] 25 mM phosphate buffer, pH 6.5, 150 mM NaCl and 37 °C, α-synuclein concentration was equal to 250 nM and L/P=200

500 s^{-1} for DOPC/DOPG 3:1, 1:1 and 1:3, respectively. The increase in k_{ex} with increasing charge content of the membrane may be due to the electrostatic repulsion between the negatively charged headgroups and negatively charged C-terminal segments of the membrane-associated α-synuclein molecules. Following this line of reasoning, C-terminally truncated α-synuclein would be expected to show different dynamics of membrane interactions. The dynamic equilibrium between the soluble and membrane-associated states is core to the peripheral membrane binding proteins' function. Deleterious effects have been observed for cases where the association of the protein with the membrane was increased as well as decreased[36]. Thus, the C-terminal segment of α-synuclein may regulate membrane association, while not participating in the binding directly.
An interesting question is whether α-synuclein binding to lipid membranes is a diffusion limited process. It was shown for multiple peripheral membrane binding proteins, which associate with membranes through different mechanisms, that the association is very fast or even diffusion limited[37,38]. Since α-synuclein is in random coil conformation in solution and folds into an α-helix upon membrane binding, the conformational transition could be the rate limiting step. The time it takes to form an α-helix is of the order of 100/N μs, where N is the number of residues that fold together[39], which gives approx. 1 μs for the case of α-synuclein. However, to the best of the author's knowledge no experimental data exists to determine which of the two events, diffusion of a protein to the surface of the vesicle or folding into an α-helix, is rate limiting.

2.6 Cooperativity of α-synuclein association with lipid membranes

In Paper III, we have studied α-synuclein distribution in excess of lipid membranes and arrived at the conclusion that the protein associates with membranes in a cooperative as opposed to an independent manner. In this section, our results will be presented and discussed alongside other reports from the literature corroborating our findings.
Cooperativity is defined as a free energy coupling between binding events. The phenomenon is present in interactions of small molecules with proteins (e.g. oxygen binding to hemoglobin) as well as in protein association with lipid membranes (e.g. self-assembly of clathrin coats in clathrin-mediated endocytosis[40] and self-assembly of dynamin at the neck of endocytic

buds[41]). Positive cooperativity means that the affinity of a ligand to a marcomolecule/membrane is higher when another ligand is already bound. This enables the regulation of processes over a narrower free ligand concentration range than would be possible in the case of independent binding.
Small molecule binding to proteins is usually deduced as cooperative or independent based on the shape of the binding curve[42], with cooperative binding giving rise to a steeper dependence of fractional saturation on ligand concentration. The characterization of protein association with membranes in such a way is much more complicated due to the unknown, but very high stoichiometry of the complex (one vesicle may be able to accommodate several hundreds or thousands of proteins). We have characterized α-synuclein binding to lipid membranes as positively cooperative based on the experimental studies of the protein distribution in the presence of the excess of lipid membranes.

Observation of non-random distribution of α-synuclein in membrane excess

We have observed non-random distribution of α-synuclein in excess of giant unilamellar vesicles using confocal microscopy and in excess of small unilamellar vesicles using fluorescence cross-correlation spectroscopy. Figure 2.14A shows a set of fluorescence and bright field images of the same region of the sample, where the fluorescently labelled α-synuclein is associated only with some of the non-labelled giant unilamellar vesicles (GUVs). The non-random distribution of the protein in a population of GUVs was ruled out to be due to incomplete mixing, differences in composition between vesicles or direct effects of membrane curvature (see Paper III).

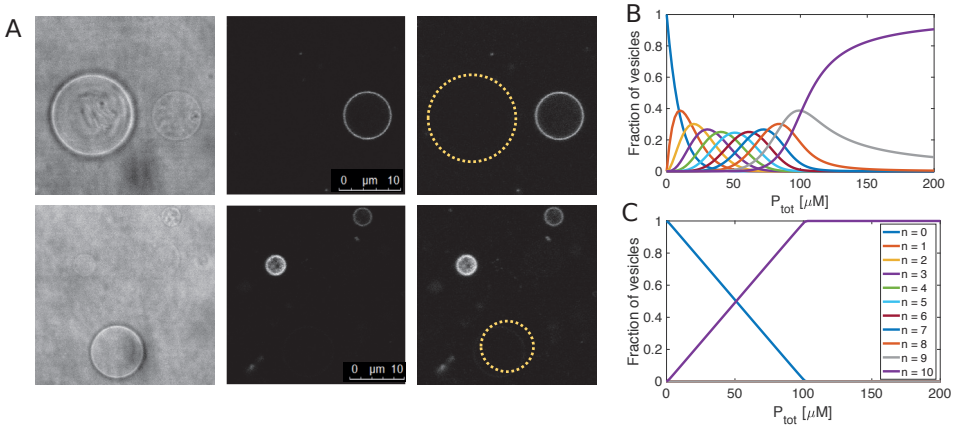

Figure 2.14 Non-random distribution of α-synuclein in a population of giant unilamellar vesicles (GUVs). A) Two sets of bright-field (left) and fluorescence mode (middle) images of non fluorescently-labelled GUVs and fluorescently labelled α-synuclein. The protein association with GUVs renders them visible in the fluorescence mode. The protein-free GUVs invisible in the fluorescence mode are marked with a yellow dotted circle in the rightmost panel. B and C) Modeling the confocal experiment results using the Adair equation (for details see Paper III). The fractions of vesicles with n occupied binding sites out of a total of 10 binding sites as a function of protein concentration (the vesicle concentration was held constant) for the cases of independent binding (B) and positively cooperative binding (C). The legend for B is the same as in C. The free energy coupling between the binding events in the latter case was -10 kJ/mol.

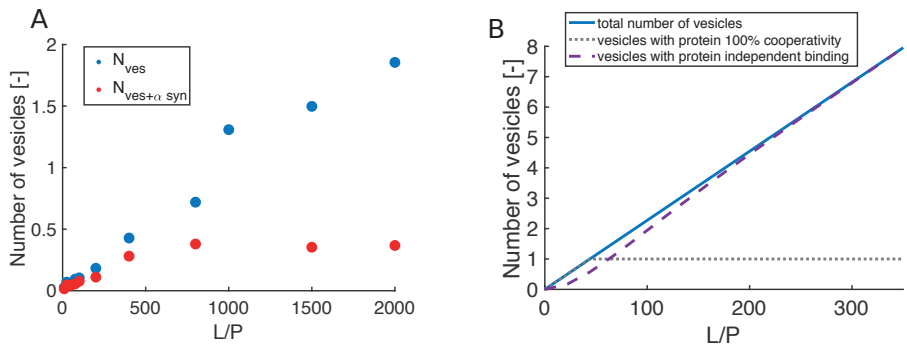

Figure 2.15 Distribution of α-synuclein in a population of small unilamellar vesicles studied with fluorescence cross-correlation spectroscopy. A) The total number of vesicles in the sample (blue dots) and the number of vesicles that have protein bound (red dots) as a function of L/P, extracted from the auto-correlation curves in the FCCS experiment. B) Modeling the FCCS results. Theoretical predictions of the number of vesicles having protein bound as a function of L/P for the cases of independent (purple dashed line) and infinitely cooperative binding (gray dotted line). The solid blue line corresponds to the total number of vesicles. In the calculations, the protein concentration was kept constant, while the lipid concentration was varied. In the case of independent binding, the number of proteins bound to each vesicle was assumed to follow a binomial distribution. In the case of infinite cooperativity, all protein molecules were assumed to occupy one vesicle regardless of the vesicle excess.

Figure 2.15A shows the total number of vesicles in the sample and the number of protein-associated vesicles extracted from the correlation curves in the fluorescence cross-correlation spectroscopy experiment. In the membrane excess regime (here L/P > 400), α-synuclein is associated with a constant number of vesicles, regardless of the extent of the membrane excess.

Box 8: How particles are counted in Fluorescence Correlation Spectroscopy?

In FCS, the fluorescence emitted by a tiny number of molecules or particles in a tiny observation volume is detected and analyzed. The raw FCS data have the form of an intensity trace (see A and B below). A spike in such an intensity trace corresponds to a fluorescent object crossing the observation volume. The width of the spike reflects how long a given object stays in the focal volume and thus provides information on its diffusion properties (long time in the focal volume = slow diffusion = big object). The height of the intensity spike reports on how many photons a given particle emitted while residing in the focus. The density of the spikes in the intensity trace provides information on the concentration of fluorescent species.

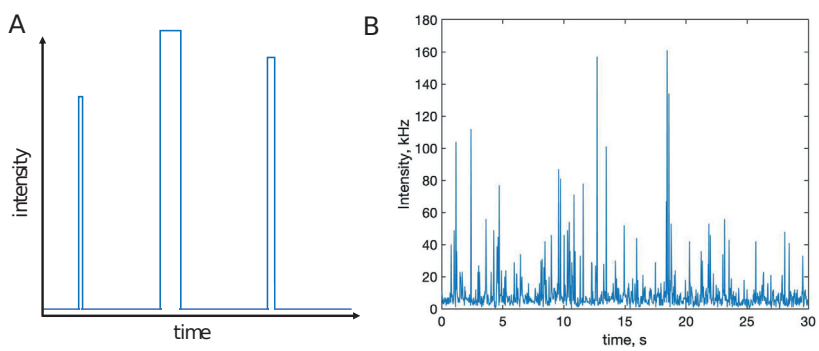

A) A schematic FCS intensity trace, in which three particles have crossed the observation volume in the time-frame of the experiment. B) An experimental intensity trace of a sample containing fluorescently labelled small unilamellar vesicles.

Modelling the experimental results

We have modelled the non-random distribution of α-synuclein in a population of GUVs that we observed in the confocal experiment using the so-called Adair equation (details in Paper III)[43]. Figure 2.14B,C shows the calculated fractions of empty (protein-free) vesicles, vesicles filled completely with protein, and all intermediate states as a function of protein concentration (vesicle concentration was kept constant) for the cases of independent binding (Figure 2.14B) and positively cooperative binding (Figure 2.14C). In the case of independent binding, the intermediate states (vesicles with 1-9 proteins bound) are populated throughout the titration. However, when a reasonable level of cooperativity is assumed (-10 kJ/mol), the intermediate states are fully suppressed and only the empty vesicles or vesicles filled completely with protein are observed. This is consistent with our observation of α-synuclein distribution in a population of GUVs in the confocal experiment.
The FCCS results presented in Figure 2.15A can be compared with the theoretical predictions of the number of vesicles with protein bound for the cases of independent and cooperative binding shown in Figure 2.15B. The calculations were carried out for vesicles with 1000 binding sites and protein concentration was set equal to the amount of protein molecules that can fill one vesicle completely. Clearly, our experimental results cannot be explained by independent binding.
The magnitude of the free energy coupling between the binding events that was sufficient to model our experimental observations, around – 10kJ/mol, is consistent with the values known for other systems involving cooperative binding[42].

Cooperativity of α-synuclein binding to membranes in the literature

Since α-synuclein association with lipid membranes has been studied extensively, it is legitimate to ask why it was not characterized as cooperative before. It turns out that multiple studies in the literature are consistent with our hypothesis and corroborate our findings. Several examples are discussed in Paper III. An additional example is included in the work of Galvagnion et al[26]. The authors studied interactions of α-synuclein with lipid vesicles using differential scanning calorimetry[26]. Samples at a range of L/P 5-200 were investigated. At lowest L/P the DSC thermogram

consisted of only the peak corresponding to protein-bound lipids, while at highest L/P only the peak corresponding to protein-free lipids appeared in the thermogram. In the intermediate L/P range both peaks were present. This indicates that the protein-free and protein-rich bilayer patches coexisted in the sample in the intermediate L/P range, rather than protein distributing homogeneously over the accessible membrane surface.

Molecular origin of cooperativity

Our study did not address the molecular mechanism underlying the cooperative binding of α-synuclein to lipid membranes; however, it must be related to the balance between the protein-protein, lipid-lipid, protein-lipid, protein-solvent and/or membrane-solvent interactions. Attractive protein-protein interactions are expected to play an important role. Additionally, when α-synuclein adsorbs and folds on the membrane, it creates a new hydrophobic interface along the α-helix. The free energy of binding of the second α-helical protein may be lower for that location as compared to the bare membrane surface. It is also possible that unfavorable effects on the lipids such as reduced lateral diffusion and thereby a decrease in entropy may be minimized if the proteins bind close to each other or in a specific pattern. The positive cooperativity may also have its origin in the interactions of the protein or membrane components with water and counter ions, with the net desolvation being more favorable for cooperative compared to isolated protein binding. Computational studies showed that peripheral membrane proteins may interact with each other through the local changes in membrane curvature, that each protein exerts upon binding[44,45]. A local curvature field induced by one bound protein may affect how the incoming proteins bind, leading to organization of the bound proteins on the membrane - a manifestation of cooperative binding.
The cooperative nature of α-synuclein association with lipid membranes is likely to be vital for the healthy function of the protein, which involves membrane remodeling. α-synuclein-induced membrane deformation will be discussed in Section 2.8.

Perspective

An interesting question is whether the Parkinson's Disease-related α-synuclein mutants also associate cooperatively with lipid membranes.

2.7 Curvature effects versus packing defects

There exist many reports in the literature showing that α-synuclein has higher affinity for vesicles of diameter below 40 nm when compared with vesicles with diameter of 100 nm or more[3,27,46,47]. Based on such reports α-synuclein was suggested to be a curvature-sensing protein. In the case of the smallest vesicles possible to obtain in the lab, surface curvature effects may be expected to play a role for a protein of α-synucllein's size (15 nm in length when bound to the membrane with the 1-100 residue segment[48]). Nevertheless, the analysis of protein binding to such small vesicles is complicated by the fact that the higher membrane curvature will impose changes in the lipid packing and may induce packing defects[46,49,50].
Shvadchak et al and Nuscher et al[27,47] studied α-synuclein association with vesicles for a range of vesicle sizes. In the case of charged membranes, α-synuclein displayed the same affinity regardless of the vesicle size (40 nm vs 100 nm diameter). However, the authors observed protein association with zwitterionic vesicles with the protein affinity increasing with decreasing vesicle size. In both studies, it was also observed that α-synuclein affinity to zwitterionic vesicles was higher when the membrane was in the gel phase when compared to the liquid crystalline state. It was concluded, that defects (sites with higher exposure of the hydrocarbon region of the bilayer) in the zwitterionic membrane may act as binding sites for α-synuclein. The smaller the vesicle (the higher the vesicle curvature), the more such defects are expected to arise, explaining the higher affinity of the protein. This conclusion is supported by the fact that when cholesterol is added to to neutral membranes, α-synuclein affinity is decreased[27]. Cholesterol has strong effect on lipid packing and was shown to eliminate defects in high curvature membranes by binding to the sites of higher exposure of the hydrocarbon core[7].
The above discussed results show that it is not easy and in some cases even impossible to distinguish between effects due to curvature of the membrane surface and due to packing defects. However, in the case of model systems such as giant unilamellar vesicles with diameter in the range of a few to a few tens of μm, it is safe to assume that the membrane surface appears flat to a protein of α-synuclein size (Figure 1C in Paper III).

2.8 α-synuclein-induced deformation of lipid membranes

Interactions with membranes are believed to be central to the healthy function of α-synuclein. The existing evidence points to the fact that the protein is involved in neurotransmitter release at the presynaptic termini[12,13], which is a process involving large-scale membrane remodeling. Thus, studies of the α-synuclein-induced membrane deformation may shed light on the healthy function of the protein.

Double anchor model

An important contribution on the membrane remodeling by α-synuclein is the work by Fusco et al[51], who based on cryo-TEM images of prolate-shaped vesicles in the presence of α-synuclein, put forward a model of α-synuclein-mediated vesicle fusion. The authors introduced a so-called "double-anchor" model, which builds on the previous works identifying multiple different α-synuclein-membrane binding modes[33]. The authors suggest that the substantially different dynamics detected in the different segments of membrane-bound α-synuclein (discussed in Section 2.4) would enable one protein molecule to associate with two vesicles at the same time. According to the model, the association with one vesicle would be mediated by a short N-terminal segment and to the second vesicle by a segment close to the C-terminus. In such a way, two vesicles would be brought to a close contact, which according to the authors would facilitate fusion. The author of this thesis expresses doubts about the legitimacy of the cryo-TEM and NMR data interpretation on which the "double-anchor" model is based. These doubts were put to a constructive use as will be described next.

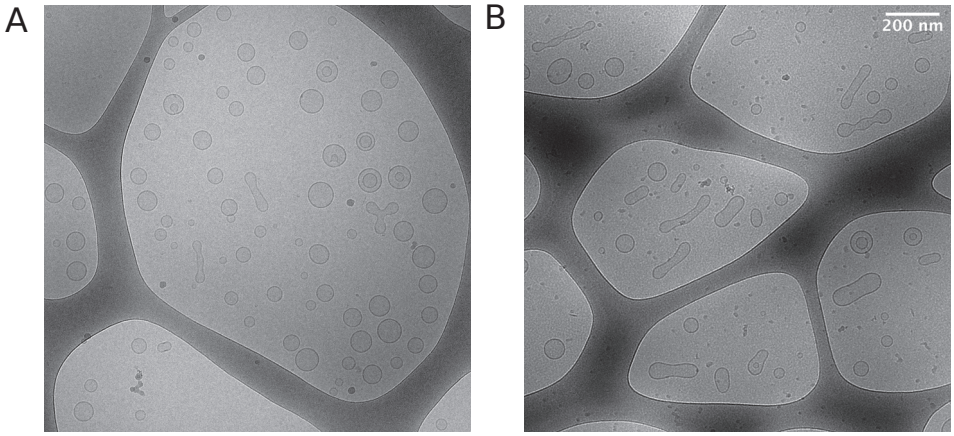

Figure 2.16 Deformation of small unilamellar vesicles composed of DOPC:DOPS 7:3 induced by α-synuclein association observed with cryo-TEM. A) Cryo-TEM image of free SUVs in 10 mM MES pH 5.5. B) Cryo-TEM image of SUVs with α-synuclein at L/P 200 24 h after the addition of the protein. The scale bar for image in A is the same as in B.

Our investigation of α-synuclein induced remodeling of model membranes described in Paper IV started with imaging of SUVs in absence and presence of α-synuclein using cryo-TEM. We observed that originally spherical vesicles undergo shape change to a prolate upon α-synuclein association, which is in line with the observations made by Fusco et al[51]. However, the fact that we observed the prolate-shaped vesicles not only shortly after the addition of the protein but also 24 hours later, prompted us to question the interpretation that they are fusion intermediates. In the work described in Paper IV, we combined cryo-TEM and fluorescence cross-correlation spectroscopy to show that the prolate structures are not fusion intermediates but are kinetically stable fission intermediates.

Fusion or fission?

First, we addressed the question whether vesicle fusion or fission occurred upon α-synuclein addition using FCCS. Figure 2.17 shows the auto- and cross-correlation curves of a sample containing a 1:1 mixture of SUVs containing a red fluorescently labelled lipid analogue and SUVs containing a green fluorescently labelled lipid analogue. The amplitudes of the auto-correlation curves are inversely proportional to the number of the respective singly-labelled species, while the amplitude of the cross-correlation curve is directly proportional to the number of doubly-labelled species (see Box 9). The numbers of green and red vesicles extracted from the auto-correlation

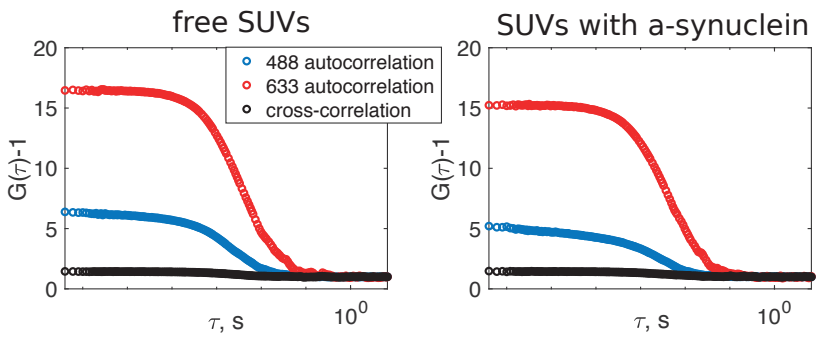

Figure 2.17 Detecting fusion or fission with fluorescence cross-correlation spectroscopy. Left: the auto- and cross-correlation curves of a sample containing a mixture of vesicles containing red fluorescent lipid analogue and vesicles containing green fluorescent lipid analogue. The amplitudes of the auto-correlation curves are inversely proportional to the amount of the respective singly labelled species. The amplitude of the cross-correlation curve is directly proportional to the amount of doubly-labelled species. Right: FCCS curves recorded for a sample containing green and red vesicles and α-synuclein at L/P 50.

curves are equal after the correction for background fluorescence from residual free dye (See Paper IV). The very low amplitude of the cross-correlation curve is consistent with the absence of doubly-labelled species in the sample. Upon the addition of α-synuclein to the vesicles, the amplitudes of the auto-correlation curves remain virtually unchanged. This implies that no detectable fission occurs, as this would lead to a higher number of singly labelled species in the sample (a decrease in the auto-correlation amplitudes). Moreover, no detectable fusion occurs as this would lead to an emergence of a population of doubly-labelled species resulting in an increase in the cross-correlation amplitude.

Box 9: Detecting doubly-labelled species in Fluorescence Cross-Correlation Spectroscopy

Figure below shows schematic intensity traces for a sample containing red particles, green particles and red-green particles. A green particle crossing the detection volume gives rise to a photon burst in the green channel, while a red particle gives rise to a photon burst in the red channel. A doubly-labelled particle diffusing through the detection volume gives rise to a photon burst in both channels. The result of an FCCS experiment is a red auto-correlation curve, a green auto-correlation curve and the cross-correlation curve. While the amplitudes of the auto-correlation functions are inversely proportional to the number of the (at least) singly-labelled particles, the amplitude of the cross-correlation function is directly proportional to the concentration of the doubly-labelled species.

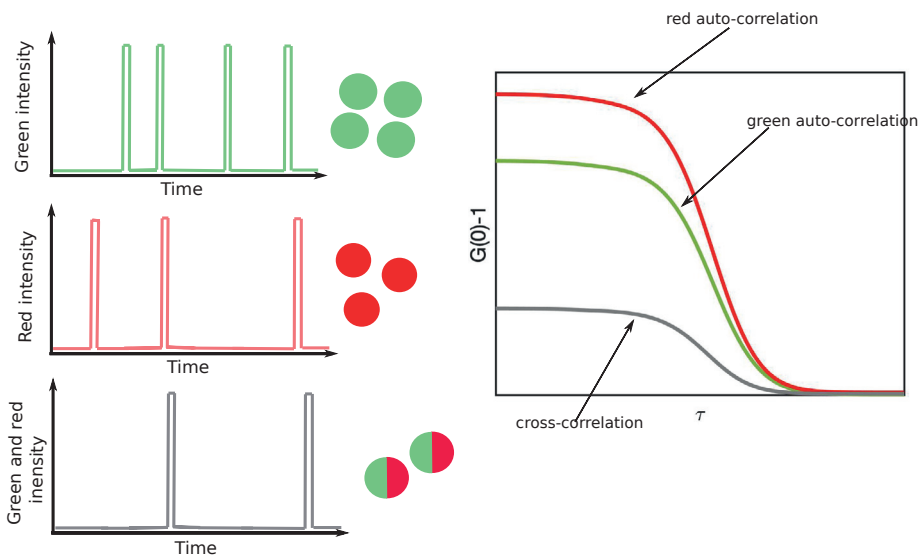

Fluorescence cross-correlation spectroscopy. Left: Schematic intensity traces for the green, red and cross-correlation channel. A doubly-labelled fluorescent particle diffusing through the focus gives rise to a signal in the cross-correlation channel. Right: A schematic FCCS dataset: two auto-correlation curves and a cross-correlation curve.

Next, we employed inverse fluorescence cross-correlation spectroscopy (iFCCS) to measure the changes in vesicle volume that occur upon α-synuclein association. For details on how the particle volume can be determined using iFCCS, see Box 10 and Figure 2.18A. As shown in Figure 2.18B, the amplitude of the anti-correlation curve measured for the sample containing SUVs and α-synuclein is lower than the amplitude of

the anti-correlation function of the sample containing only vesicles. This implies that the vesicle volume decreases upon α-synuclein association. The volume decrease could be interpreted as being due to vesicle fission, but the FCCS results ruled out that any detectable fission occurs. However, the observed decrease in vesicle volume upon α-synuclein addition is consistent with the change in shape from a sphere to a prolate occurring at a fixed membrane surface area.

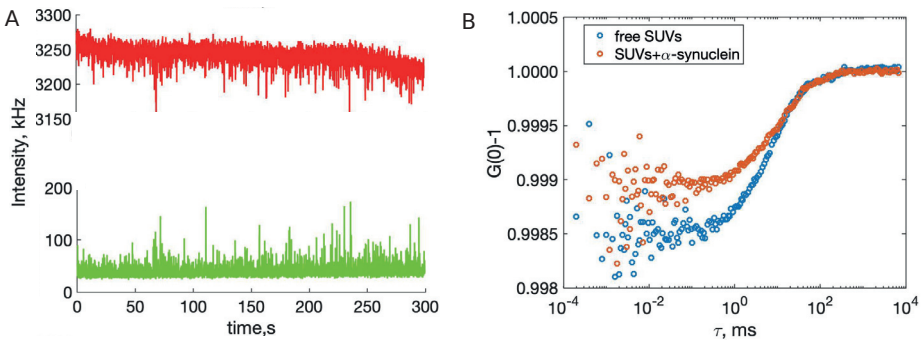

Figure 2.18 Determining the vesicle volume change upon deformation with inverse fluorescence cross-correlation spectroscopy. SUVs contained a green fluorescent lipid analogue and 100 μM of red fluorescent dye was dissolved in the solvent. Since the dye does not penetrate the membrane, a vesicle diffusing through the focal volume, displaces some of the dye molecules. This gives rise to a negative signal in the red intensity trace. At the same time, the vesicle gives rise to a positive signal in the green intensity trace. The signals from the two channels are cross-correlated giving rise to an anti-correlation curve as shown in B. The amplitude of the anti correlation curve is proportional to the volume of the particle that displaces the dye molecules from the focus. The iFCCS amplitudes measured on free SUVs and SUVs with α-synuclein show that the volume of the vesicle decreases upon protein association.

Box 10: How particle volume is determined in Inverse Fluorescence Cross-Correlation spectroscopy

In inverse Fluorescence Correlation Spectroscopy, the parameter of interest is not the fluorescence intensity fluctuations due to a diffusing fluorescent molecule or particle of interest (as in conventional FCS), but the intensity fluctuations due to the surrounding medium[52]. This requires that a relatively high amount of fluorescent dye is dissolved in the medium. At a high dye concentration, at all times throughout the experiment, there are some dye molecules in the focus, which give rise to a high signal in the intensity trace. A particle (such as a vesicle) diffusing through a focus displaces some of the dye molecules giving rise to a negative signal in the intensity trace (as in the red trace in Figure 2.18A).

In the inverse Fluorescence Cross-Correlation Spectroscopy (iFCCS), the particle displacing the dye is also fluorescently labelled. Thus, the negative signal from the displaced dye can be cross-correlated with the positive signal coming from the particle detected in the second channel, which gives rise to an anti-correlation curve (Figure 2.18B). The amplitude of this curve is directly proportional to the volume of the particle displacing the dye molecules. The derivation of the relation between the amplitude of the iFCCS curve and the volume of the particle is presented in Supplementary Information of Paper IV.

Driving force for deformation

The fact that the vesicle deformation persists for extended periods of time after the addition of α-synuclein, as observed with cryo-TEM, implies that the deformed vesicle is a kinetically stable state, although it might not be thermodynamically stable. Moreover, the persistence of the pearl-on-a-necklace structures implies that there is a driving force to increase the curvature of the membrane. The origin of this driving force can be ascribed to the protein adsorption. The adsorption of α-synuclein molecules on the outer leaflet of a vesicle induces higher positive spontaneous curvature than the spontaneous curvature of an empty vesicle[53]. A way to relax this elastic energy would be that a vesicle undergoes fission. Fission is however a process involving a disruption of membrane continuity and thus involving a high energy barrier, which apparently cannot be overcome by thermal fluctuations in the experimental time-frame at the conditions of our experiment. The deformed vesicles reminiscent of a pearl-on-a-necklace are therefore most possibly kinetically stable fission intermediates.

Perspective

An interesting aspect of the protein adsorption-mediated membrane remodeling is protein organization on the membrane. The binding energies between a protein and a lipid are much lower than the energy required for large-scale changes in membrane geometry[54,55]. This implies that cooperative action of many proteins is necessary for membrane remodeling on mesoscale. Protein self-assembly on the membrane is well studied in the context of e.g. clathrin-mediated endocytosis, where multiple proteins form so-called "coats" on the membrane and induce bending. Self-assembly of α-synuclein on a membrane is a new concept, which requires further studies to be better understood. It is however consistent with the finding that α-synuclein associates with membranes in a cooperative manner.

2.9 α-synuclein amyloid formation in presence of lipid membranes

In the previous chapters, we discussed α-synuclein interactions with lipid membranes in conditions, where no amyloid fibril formation occurred (or before it occurred). Those insights are most possibly vital to understand the healthy function of the protein. It will however be fair to say that α-synuclein attracts more attention in the context of its aberrant aggregation associated with neurodegenerative diseases. α-synuclein amyloid fibrils were initially thought to be the main component of the Lewy Bodies, which are intraneuronal inclusions being a hallmark of Parkinson's Disease[56]. Later, it was recognized that Lewy Bodies contain a large proportion of crowded lipid membranes[57]. This motivated the studies of α-synuclein amyloid formation in the presence of membranes, some of the most important conclusions from which will be discussed in this chapter.

The effect of relative amounts of proteins and lipids

The effect that the presence of lipid membranes has on α-synuclein aggregation ranges from acceleration to inhibition and was shown to depend on the relative proportions of the protein and lipids[58]. We have investigated

this in Paper I. In a system consisting of small unilamellar vesicles and initially monomeric α-synuclein, the aggregation is accelerated at low L/P and inhibited at high L/P as shown in Figure 2.19. At low membrane content (low L/P), apart from the protein associated with the vesicle, there is a substantial population of free protein in solution. At high L/P, since the equilibrium between the free and vesicle-associated protein is strongly shifted towards the complex, virtually all protein is bound (Figures 2, 3, 5 in Paper I and Figure 4C in Paper II). The dependence of the effect of membranes on α-synuclein aggregation suggests that for the aggregation to occur, free and vesicle-associated protein need to coexist.

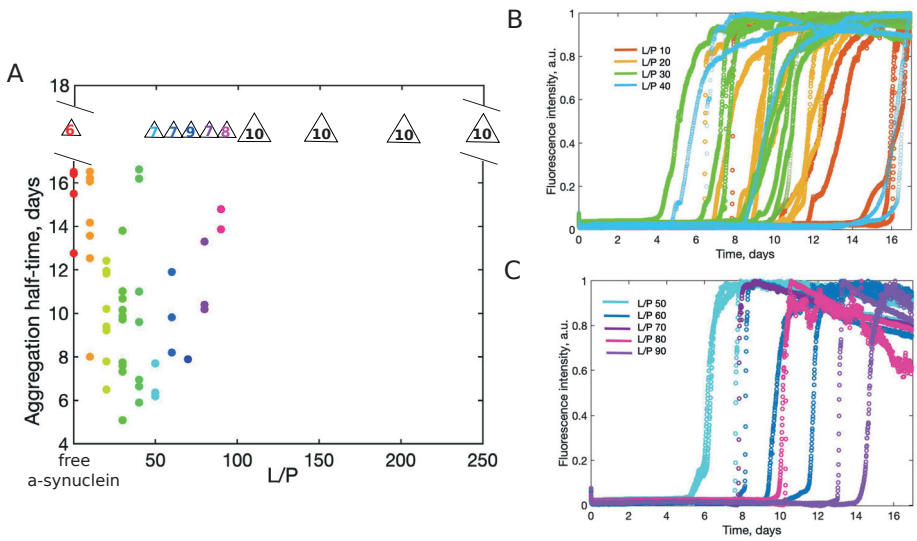

Figure 2.19 Aggregation of α-synuclein in the presence of DOPC:DOPS 7:3 SUVs at pH 5.5. A) The half-times from the ThT aggregation assay (see Box 11) for samples containing α-synuclein and SUVs at L/P ratios in the range 10-250. For each sample, 10 replicates were measured. The number in the triangles above the data points represents the number of replicates for which no aggregation was detected in the timeframe of the experiment (18 days). B) ThT intensity traces for samples at L/P 10-40. C) ThT intensity traces for samples at L/P 50-90. No aggregation was detected for samples at L/P $\geq$ 100.

Box 11: Thioflavin T aggregation kinetics assay

A standard method to follow the formation of amyloid fibrils *in vitro* involves a fluorescent molecule thioflavin T (ThT). As shown below, a ThT molecule contains a benzothioazole and a benzyl ring connected by a single $C-C$ bond. When in solution, the two rings rotate freely with respect to each other, which lowers the fluorescence quantum yield. As ThT binds to the cross-beta structure of the amyloid fibrils, the molecule becomes more rigid and the quantum yield increases. In an aggregation kinetics assay, the protein is incubated with ThT and an increase in the ThT emission is indicative of an increase in the fibril mass, provided that the assay is properly optimized in terms of the total ThT concentration and the ThT/protein ratio.

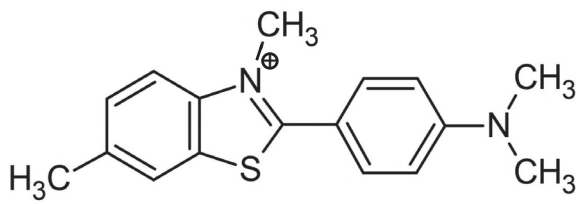

Thiflavin T structure.

Microscopic processes in membrane-assisted fibril formation

The microscopic processes that underlie many self-assembly processes where ordered structures form, such as crystallization and amyloid fibril formation, are primary nucleation (homogeneous and heterogeneous), secondary nucleation, growth and fragmentation. Which of those mechanisms dominates depends on many factors, including the presence of surfaces and their properties as well as the solution conditions.

In a pure protein sample, the inevitable step necessary for fibril formation is the homogeneous primary nucleation, assuming no interface effects (an idealized case). A nucleus in this context can be defined as the monomer assembly, for which it is more favorable to grow by addition of more monomers than to dissociate. A process where a nucleus forms on some interface is called heterogeneous primary nucleation. Galvagnion et al[58] showed that the rate of primary nucleation in α-synuclein amyloid fibril formation can be increased by three orders of magnitude in presence of charged lipid membranes. The enhancement of the primary nucleation rate may be due to an

increased local concentration of α-synuclein on the membrane and/or to a shift in the conformational space of the protein to an ensemble of conformations compatible with the nucleation process.
An important finding in this context is that the amount of α-synuclein converted into fibrils does not depend on the initial amount of free protein in solution, but on the amount of protein initially bound to the membrane[58]. Figure 2.20 shows the dependence of the amount of α-synuclein converted into fibrils for the cases of constant concentration of lipid vesicles and increasing protein concentration (Figure 2.20 A) and increasing concentration of lipid vesicles and constant protein concentration (Figure 2.20 B). The data shows that at constant lipid concentration, a constant amount of α-synuclein is converted into fibrils, regardless of the amount of excess free protein in solution. This implies that secondary nucleation does not contribute to the fibril formation as in such a case one would expect that the total amount of protein converted into fibrils would depend on the initial free protein concentration. This result also shows that the aggregation process does not stop due to the depletion of free protein from the solution. The mechanistic details of what happens on the surface of the vesicle in the membrane-assisted α-synuclein aggregation remain elusive, however some important aspects of the process are discussed in the following subsection.

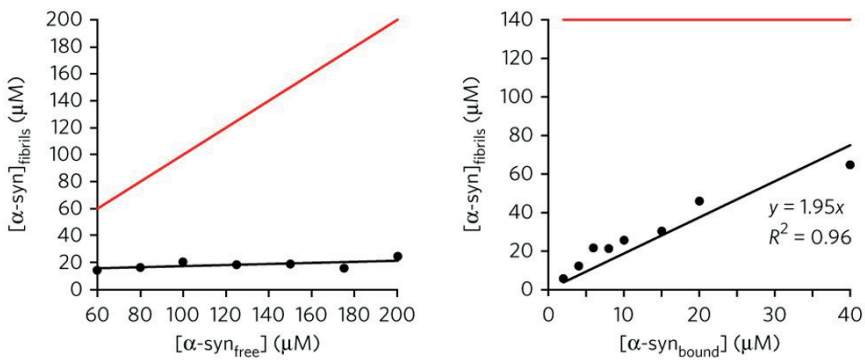

Figure 2.20 Effect of the variation of the concentration of vesicles and free α-synuclein on the total mass of the protein converted into fibrils. A) The total concentration of α-synuclein converted into fibrils in the presence of a constant amount of vesicles and increasing initial concentration of the monomer (black). The fact the amount of vesicles was kept constant implies that the amount of membrane-associated protein was the same in all samples. The L/P range covered is 3.3-1.5. B) The total concentration of α-synuclein converted into fibrils in presence of an increasing amount of lipid vesicles and constant initial amount of monomeric α-synuclein (black). The L/P range covered is 0.4-8.6. The red lines in A and B, show the expected trend of the total protein mass converted into fibrils if secondary processes dominated fibril formation. Adapted with permission from reference[58].

The role of electrostatics

Even though hydrophobic interaction is the main driving force for protein aggregation, the short-range electrostatic attractions were shown to be critical for both the secondary nucleation of α-synuclein on a surface of existing fibrils and the heterogeneous primary nucleation on the surface of α-synuclein-covered membrane[59]. In the following discussion, the focus will be on the latter process. The same principles are however expected to apply in both cases.

Gaspar et al investigated the effect of ionic strength on α-synuclein amyloid formation in the L/P regime, where the process in accelerated in the presence of membranes at low ionic strength[59].[iii] At high ionic strength (140 mM NaCl), no aggregation was detected. The authors performed Monte Carlo simulations to gain an insight into how α-synuclein monomer interacts with a surface grafted with α-synuclein C-terminal segments at different ionic strength conditions (the snapshot from a simulation is shown in Figure 2.21C). The extracted α-synuclein mass centre distribution function with respect to the surface show that at high ionic strength the protein is repelled from the surface (Figure 2.21A). At low ionic strength, the results indicate the presence of attractive inter-molecular interactions. Moreover, it was found that at low ionic strength α-synuclein monomer has a preferred alignment with respect to the C-terminal segments on the surface (positively charged part of the monomer interacts with the negatively charged C-termini). At high ionic strength, the monomer dipole displays no preferred orientation (Figure 2.21B).

The specific alignment of an α-synuclein monomer with respect to the C-terminal segments of the membrane-bound protein molecules is thus expected to play a critical role in the amyloid formation process. The different α-synuclein membrane-binding modes described in Section 2.3, result in different surface properties of a protein-covered membrane, with longer chains extending into the solution at low L/P than at high L/P. This is expected to affect the alignment of an incoming α-synuclein molecule, and thus affect whether the membrane accelerates or inhibits aggregation.

[iii] Lipid system: DOPC:DOPS 9:1, 10 mM MES pH 5.5, L/P 0 - 25.

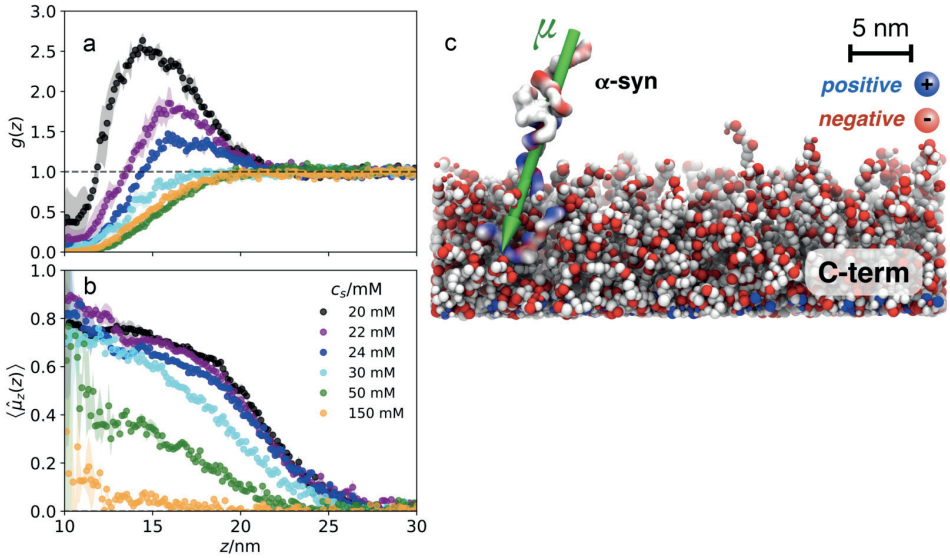

Figure 2.21 Monte Carlo simulations of the interaction of an α-synuclein monomer with a surface grafted with the C-terminal segments of the protein (residues 100-140). A) Mass centre density of α-synuclein monomer relative to bulk as a function of distance, z, to the surface grafted with α-synuclein C-terminal segments at different ionic strength. B) The degree of monomer dipole moment orientation with respect to the surface at different ionic strengths. C) A snapshot from one simulation. The green arrow represents the molecular dipole moment vector of an α-synuclein monomer. The grafted layer of C-terminal segments in represented by red/white/blue beads. Reproduced with permission from[59].

The role of lipid properties

Lipid properties such as length of the hydrocarbon chains were shown to influence the effect that membranes have on α-synuclein amyloid formation. Galvagnion et al[26] studied the effect of membranes composed of different lipid species on α-synuclein aggregation. Although, in this study α-synuclein was shown to associate with all studied membranes that were in a liquid crystalline state (DLPS, DMPS, DOPS), only membranes composed of the lipid species with shortest acyl chains (highest solubility), DLPS and DMPS, accelerated α-synuclein aggregation [iv]. Moreover, the kinetics of amyloid formation in presence of DLPS membranes (100 nM solubility) were faster than in the presence of DMPS membranes (10 nM solubility). This implies that at least part of the free energy barrier for the aggregation process in these model systems is related to the transfer of the lipid molecules from a membrane to a protein environment. This suggests

[iv] Conditions of the experiment: 20 mM sodium phosphate buffer pH 6.5, the timeframe of the experiment was around 2 days

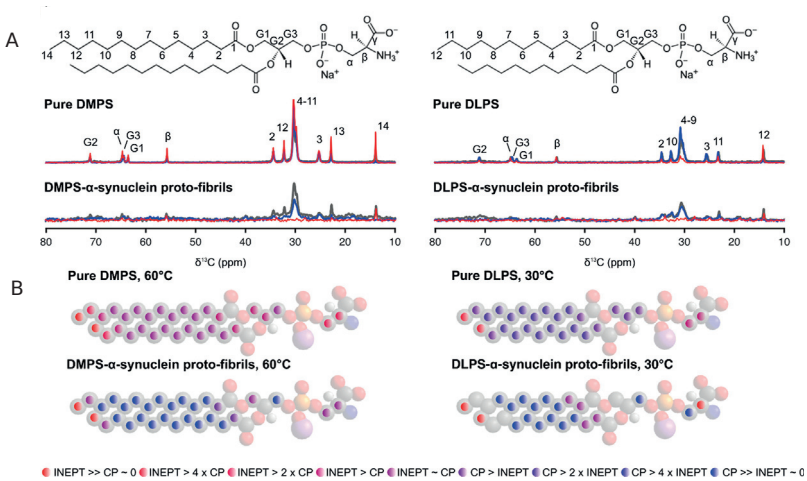

Figure 2.22 The presence of lipid molecules and their dynamics within α-synuclein aggregates probed with ^{13}C MAS NMR. A) ^{13}C CP-DP-INEPT MAS spectra of α-synuclein-DMPS and α-synuclein-DLPS co-aggregates. The CP, DP and INEPT spectra are plotted in blue, grey and red, respectively. The spectra of the co-aggregates contain resonances corresponding to carbon atoms in the lipid molecules. The numbers above the spectrum indicate which carbon atoms from the lipid give rise to a given peak. B) A cartoon representing the site-specific dynamics of lipid molecules within the α-synuclein-lipid co-aggregates. Highest INEPT intensity corresponds to the most mobile segments, while highest CP intensity corresponds to the most rigid segments of the lipid molecules. For details on CP-DP-INEPT see Box 5. Reproduced with permission from reference[60].

that the membrane does not only play a role of a surface in the aggregation process, but that the lipid molecules may be incorporated into the protein aggregates.

Incorporation of lipid molecules into α-synuclein aggregates

The question whether the lipids get incorporated into the α-synuclein aggregates was addressed in Paper VI using NMR and DSC. ^{13}C Magic Angle Spinning (MAS) NMR spectra of the protein aggregates formed in the presence of DMPS and DLPS lipid vesicles contained the resonances corresponding to lipid carbons, implying that the lipid molecules get incorporated into the amyloid fibrils (Figure 2.22A).

Site-specific dynamics of lipids within the co-aggregates

Having established that DMPS and DLPS lipid molecules get incorporated into the α-synuclein fibrils, polarization transfer ^{13}C MAS was employed to get insights into the site-specific molecular dynamics of the lipid chains, while ^{31}P MAS NMR was employed to study the dynamics of the lipid headgroups within the protein-lipid co-assemblies (Paper VI).
The cartoons in Figure 2.22B summarize the polarization transfer ^{13}C MAS results. By comparing the relative intensities of the CP, DP and INEPT signals (see Box 5), we found that all carbons in the lipid acyl chain except the end methyls have a lower reorientation rate (corresponding to an increase in correlation time) and/or a more anisotropic reorientation in the α-synuclein-lipid co-assemblies as compared to the pure lipid phase. The end methyls have a high reorientation rate and isotropic reorientation in both the co-assemblies and pure lipid phase. ^{31}P MAS NMR results showed that α-synuclein-lipid co-assembly results in slower and more isotropic reorientation of the lipid headgroup (Figure 3A in Paper VI).

Thermotropic properties of lipids with the co-aggregates

In the same study (Paper VI), we analyzed the changes in the thermotropic properties of lipids upon α-synuclein-lipid co-aggregation. We have acquired DSC thermograms of a sample containing DMPS-α-synuclein co-aggregates and the pure DMPS SUVs (Figure 2.23). The DSC thermograms showed that both the temperature and the enthalpy of the chain melting transition decreased upon co-aggregation (the temperature decreased from 39 to 29°C and the enthalpy decreased from 25 to 6 kJ/mol). We also treated the protein-lipid sample with unspecific protease, proteinase K, and acquired a DSC thermogram. The protease cleaves the peptide bonds in the protein chain, resulting in single amino acids and short peptides. In the protease-treated sample, the peak in the DSC thermogram appeared at 39°C as is the case of pure lipid vesicles. The enthalpy of this transition was equal to around 70% of the enthalpy measured for a pure vesicle sample, implying that the treatment with pK releases the lipid molecules from the aggregates. These results corroborate the ^{13}C MAS result that the lipid molecules are incorporated into the protein aggregates. The decrease in the transition temperature in the co-aggregates vs pure lipid phase can be explained by that the lipid molecules are more ordered at low temperatures and/or more rigid at high temperatures in the co-aggregates as compared to the pure lipid phase. Based on the results presented in Paper VI, we

cannot determine whether the lipid molecules are incorporated into the co-aggregates as individual molecules, lipid monolayers or bilayers.

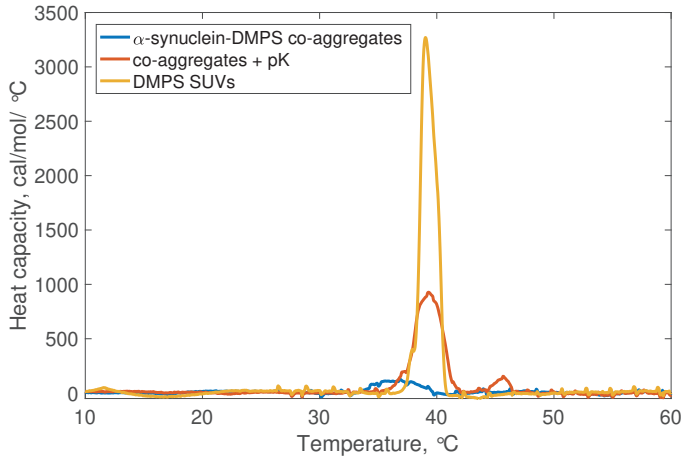

Figure 2.23 Differential Scanning Calorimetry on free DMPS SUVs (yellow), α-synuclein-DMPS co-aggregates (blue) and α-synuclein-DMPS co-aggregates treated with proteinase K (orange). For details on the digestion protocol see Paper VI.

pH dependence of the effect of membranes on α-synuclein aggregation

α-synuclein aggregation in the presence of lipid membranes was studied at different solution conditions. At pH 6.5, the vesicles composed of lipids with short acyl chains, DMPS (14 carbon acyl chains) and DLPS (12 carbon acyl chains), had an accelerating effect on α-synuclein amyloid formation, while vesicles composed of lipids with longer acyl chains, such as DOPS, had no effect. In Paper I, we have studied α-synuclein aggregation in presence of DOPC:DOPS 7:3 vesicles at pH 5.5 and found that amyloid formation was accelerated in the low L/P range (10-80) and inhibited at higher L/P (Figure 2.19). The important difference between the aggregation assays carried out by us and by Galvagnion et al is the time-frame of the experiment - 3 weeks and 1 week, respectively. Thus, the observation of no effect of DOPS membranes on α-synuclein aggregation at pH 6.5 within one week may be due to either slower aggregation kinetics in the presence of membranes of this type when compared to DLPS or DMPS membranes or to the fact that at such pH the DOPS membranes actually have an inhibiting effect on α-synuclein aggregation. Which of the two is the case remains an open question.

Perspective

Event though the fast kinetics of α-synuclein aggregation in the presence of membranes composed of lipid species with short acyl chains such as DLPS and DMPS, make it a good model system, it should be emphasized that these are not the lipid species forming membranes *in vivo*. The lipid species found in biological membranes have longer acyl chains (18-22 carbon atoms). The properties of DMPS and DLPS are much different from the more biologically relevant lipid species (e.g. DOPC, DOPS). The short chain endows the lipid molecule with much higher solubility in water. Also, DMPS and DLPS tend to form different supra-molecular structures than the lipid species with longer chains. The results presented above should be considered a starting point towards better understanding of α-synuclein amyloid fibril formation in the presence of membranes composed biologically relevant lipid species. However, it should be borne in mind that the behavior of the system containing lipid species with longer acyl chains may be substantially different.

References

[1] Wright, P. E.; Dyson, H. J. Intrinsically unstructured proteins: re-assessing the protein structure-function paradigm. *Journal of molecular biology* **1999**, *293*, 321–331.

[2] Uversky, V. N. Unusual biophysics of intrinsically disordered proteins. *Biochimica et Biophysica Acta (BBA)-Proteins and Proteomics* **2013**, *1834*, 932–951.

[3] Davidson, W. S.; Jonas, A.; Clayton, D. F.; George, J. M. Stabilization of α-synuclein secondary structure upon binding to synthetic membranes. *Journal of Biological Chemistry* **1998**, *273*, 9443–9449.

[4] Ulmer, T. S.; Bax, A.; Cole, N. B.; Nussbaum, R. L. Structure and dynamics of micelle-bound human α-synuclein. *Journal of Biological Chemistry* **2005**, *280*, 9595–9603.

[5] Wang, C.; Shah, N.; Thakur, G.; Zhou, F.; Leblanc, R. M. α-Synuclein in α-helical conformation at air–water interface: implication of conformation and orientation changes during its accumulation/aggregation. *Chemical communications* **2010**, *46*, 6702–6704.

[6] Devaux, P.; McConnell, H. Lateral diffusion in spin-labeled phosphatidylcholine multilayers. *Journal of the American Chemical Society* **1972**, *94*, 4475–4481.

[7] Mouritsen, O. G.; Bagatolli, L. A. *Life-as a matter of fat: lipids in a membrane biophysics perspective*; Springer, 2015.

[8] Zong, W.; Li, Q.; Zhang, X.; Han, X. Deformation of giant unilamellar vesicles under osmotic stress. *Colloids and Surfaces B: Biointerfaces* **2018**, *172*, 459–463.

[9] Pencer, J.; White, G. F.; Hallett, F. R. Osmotically induced shape changes of large unilamellar vesicles measured by dynamic light scattering. *Biophysical journal* **2001**, *81*, 2716–2728.

[10] Lücking, C.; Brice, A. Alpha-synuclein and Parkinson's disease. *Cellular and Molecular Life Sciences CMLS* **2000**, *57*, 1894–1908.

[11] Burré, J. The synaptic function of α-synuclein. *Journal of Parkinson's disease* **2015**, *5*, 699–713.

[12] Liu, S.; Ninan, I.; Antonova, I.; Battaglia, F.; Trinchese, F.; Narasanna, A.; Kolodilov, N.; Dauer, W.; Hawkins, R. D.; Arancio, O. α-Synuclein produces a long-lasting increase in neurotransmitter release. *The EMBO journal* **2004**, *23*, 4506–4516.

[13] Cheng, F.; Vivacqua, G.; Yu, S. The role of alpha-synuclein in neurotransmission and synaptic plasticity. *Journal of chemical neuroanatomy* **2011**, *42*, 242–248.

[14] Meade, R. M.; Fairlie, D. P.; Mason, J. M. Alpha-synuclein structure and Parkinson's disease–lessons and emerging principles. *Molecular neurodegeneration* **2019**, *14*, 1–14.

[15] Segrest, J. P.; Jones, M. K.; De Loof, H.; Brouillette, C. G.; Venkatachalapathi, Y.; Anantharamaiah, G. The amphipathic helix in the exchangeable apolipoproteins: a review of secondary structure and function. *Journal of lipid research* **1992**, *33*, 141–166.

[16] Peter, B. J.; Kent, H. M.; Mills, I. G.; Vallis, Y.; Butler, P. J. G.; Evans, P. R.; McMahon, H. T. BAR domains as sensors of membrane curvature: the amphiphysin BAR structure. *Science* **2004**, *303*, 495–499.

[17] Simunovic, M.; Voth, G. A.; Callan-Jones, A.; Bassereau, P. When physics takes over: BAR proteins and membrane curvature. *Trends in cell biology* **2015**, *25*, 780–792.

[18] Fusco, G.; Sanz-Hernandez, M.; De Simone, A. Order and disorder in the physiological membrane binding of α-synuclein. *Current opinion in structural biology* **2018**, *48*, 49–57.

[19] Hellstrand, E.; Grey, M.; Ainalem, M.-L.; Ankner, J.; Forsyth, V. T.; Fragneto, G.; Haertlein, M.; Dauvergne, M.-T.; Nilsson, H.; Brundin, P., et al. Adsorption of α-synuclein to supported lipid bilayers: positioning and role of electrostatics. *ACS chemical neuroscience* **2013**, *4*, 1339–1351.

[20] Pfefferkorn, C. M.; Heinrich, F.; Sodt, A. J.; Maltsev, A. S.; Pastor, R. W.; Lee, J. C. Depth of α-synuclein in a bilayer determined by fluorescence, neutron reflectometry, and computation. *Biophysical journal* **2012**, *102*, 613–621.

[21] Chandra, S.; Chen, X.; Rizo, J.; Jahn, R.; Südhof, T. C. A broken α-helix in folded α-synuclein. *Journal of Biological Chemistry* **2003**, *278*, 15313–15318.

[22] Burré, J.; Sharma, M.; Südhof, T. C. α-Synuclein assembles into higher-order multimers upon membrane binding to promote SNARE complex formation. *Proceedings of the National Academy of Sciences* **2014**, *111*, E4274–E4283.

[23] Georgieva, E. R.; Ramlall, T. F.; Borbat, P. P.; Freed, J. H.; Eliezer, D. The lipid-binding domain of wild type and mutant α-synuclein: compactness and interconversion between the broken and extended helix forms. *Journal of Biological Chemistry* **2010**, *285*, 28261–28274.

[24] Lokappa, S. B.; Ulmer, T. S. α-Synuclein populates both elongated and broken helix states on small unilamellar vesicles. *Journal of Biological Chemistry* **2011**, *286*, 21450–21457.

[25] Ferreon, A. C. M.; Gambin, Y.; Lemke, E. A.; Deniz, A. A. Interplay of α-synuclein binding and conformational switching probed by single-molecule fluorescence. *Proceedings of the National Academy of Sciences* **2009**, *106*, 5645–5650.

[26] Galvagnion, C.; Brown, J. W.; Ouberai, M. M.; Flagmeier, P.; Vendruscolo, M.; Buell, A. K.; Sparr, E.; Dobson, C. M. Chemical properties of lipids strongly affect the kinetics of the membrane-induced aggregation of α-synuclein. *Proceedings of the National Academy of Sciences* **2016**, *113*, 7065–7070.

[27] Shvadchak, V. V.; Falomir-Lockhart, L. J.; Yushchenko, D. A.; Jovin, T. M. Specificity and kinetics of α-synuclein binding to model membranes determined with fluorescent excited state intramolecular proton transfer (ESIPT) probe. *Journal of Biological Chemistry* **2011**, *286*, 13023–13032.

[28] Wang, M.; Mihut, A. M.; Rieloff, E.; Dabkowska, A. P.; Månsson, L. K.; Immink, J. N.; Sparr, E.; Crassous, J. J. Assembling responsive microgels at responsive lipid membranes. *Proceedings of the National Academy of Sciences* **2019**, *116*, 5442–5450.

[29] Bohon, R. L.; Claussen, W. The solubility of aromatic hydrocarbons in water1. *Journal of the American Chemical Society* **1951**, *73*, 1571–1578.

[30] Kučerka, N.; Nieh, M.-P.; Katsaras, J. Fluid phase lipid areas and bilayer thicknesses of commonly used phosphatidylcholines as a function of temperature. *Biochimica et Biophysica Acta (BBA)-Biomembranes* **2011**, *1808*, 2761–2771.

[31] Wei, Y.; Thyparambil, A. A.; Latour, R. A. Protein helical structure determination using CD spectroscopy for solutions with strong background absorbance from 190 to 230 nm. *Biochimica et Biophysica Acta (BBA)-Proteins and Proteomics* **2014**, *1844*, 2331–2337.

[32] Bodner, C. R.; Dobson, C. M.; Bax, A. Multiple tight phospholipid-binding modes of α-synuclein revealed by solution NMR spectroscopy. *Journal of molecular biology* **2009**, *390*, 775–790.

[33] Fusco, G.; De Simone, A.; Gopinath, T.; Vostrikov, V.; Vendruscolo, M.; Dobson, C. M.; Veglia, G. Direct observation of the three regions in α-synuclein that determine its membrane-bound behaviour. *Nature communications* **2014**, *5*, 1–8.

[34] Nowacka, A.; Bongartz, N.; Ollila, O.; Nylander, T.; Topgaard, D. Signal intensities in 1H–13C CP and INEPT MAS NMR of liquid crystals. *Journal of Magnetic Resonance* **2013**, *230*, 165–175.

[35] Keeler, J. *Understanding NMR spectroscopy*; John Wiley & Sons, 2011.

[36] Johnson, J. E.; Cornell, R. B. Amphitropic proteins: regulation by reversible membrane interactions. *Molecular membrane biology* **1999**, *16*, 217–235.

[37] Krishnaswamy, S.; Jones, K. C.; Mann, K. G. Prothrombinase complex assembly. Kinetic mechanism of enzyme assembly on phospholipid vesicles. *Journal of Biological Chemistry* **1988**, *263*, 3823–3834.

[38] Arbuzova, A.; Wang, J.; Murray, D.; Jacob, J.; Cafiso, D. S.; McLaughlin, S. Kinetics of interaction of the myristoylated alanine-rich C kinase substrate, membranes, and calmodulin. *Journal of Biological Chemistry* **1997**, *272*, 27167–27177.

[39] Kubelka, J.; Hofrichter, J.; Eaton, W. A. The protein folding 'speed limit'. *Current opinion in structural biology* **2004**, *14*, 76–88.

[40] Saleem, M.; Morlot, S.; Hohendahl, A.; Manzi, J.; Lenz, M.; Roux, A. A balance between membrane elasticity and polymerization energy sets the shape of spherical clathrin coats. *Nature communications* **2015**, *6*, 1–10.

[41] Roux, A.; Koster, G.; Lenz, M.; Sorre, B.; Manneville, J.-B.; Nassoy, P.; Bassereau, P. Membrane curvature controls dynamin polymerization. *Proceedings of the National Academy of Sciences* **2010**, *107*, 4141–4146.

[42] Forsén, S.; Linse, S. Cooperativity: over the Hill. *Trends in biochemical sciences* **1995**, *20*, 495–497.

[43] Adair, G. S., et al. The hemoglobin system VI. The oxygen dissociation curve of hemoglobin. *Journal of Biological Chemistry* **1925**, *63*, 529–545.

[44] Simunovic, M.; Srivastava, A.; Voth, G. A. Linear aggregation of proteins on the membrane as a prelude to membrane remodeling. *Proceedings of the National Academy of Sciences* **2013**, *110*, 20396–20401.

[45] Braun, A. R.; Lacy, M. M.; Ducas, V. C.; Rhoades, E.; Sachs, J. N. α-Synuclein-induced membrane remodeling is driven by binding affinity, partition depth, and interleaflet order asymmetry. *Journal of the American Chemical Society* **2014**, *136*, 9962–9972.

[46] Middleton, E. R.; Rhoades, E. Effects of curvature and composition on α-synuclein binding to lipid vesicles. *Biophysical journal* **2010**, *99*, 2279–2288.

[47] Nuscher, B.; Kamp, F.; Mehnert, T.; Odoy, S.; Haass, C.; Kahle, P. J.; Beyer, K. α-Synuclein has a high affinity for packing defects in a bilayer membrane: a thermodynamics study. *Journal of Biological Chemistry* **2004**, *279*, 21966–21975.

[48] Braun, A. R.; Lacy, M. M.; Ducas, V. C.; Rhoades, E.; Sachs, J. N. α-Synuclein's uniquely long amphipathic helix enhances its membrane binding and remodeling capacity. *The Journal of membrane biology* **2017**, *250*, 183–193.

[49] Ouberai, M. M.; Wang, J.; Swann, M. J.; Galvagnion, C.; Guilliams, T.; Dobson, C. M.; Welland, M. E. α-Synuclein senses lipid packing defects and induces lateral expansion of lipids leading to membrane remodeling. *Journal of Biological Chemistry* **2013**, *288*, 20883–20895.

[50] Garten, M.; Prévost, C.; Cadart, C.; Gautier, R.; Bousset, L.; Melki, R.; Bassereau, P.; Vanni, S. Methyl-branched lipids promote the membrane adsorption of α-synuclein by enhancing shallow lipid-packing defects. *Physical Chemistry Chemical Physics* **2015**, *17*, 15589–15597.

[51] Fusco, G.; Pape, T.; Stephens, A. D.; Mahou, P.; Costa, A. R.; Kaminski, C. F.; Schierle, G. S. K.; Vendruscolo, M.; Veglia, G.; Dobson, C. M., et al. Structural basis of synaptic vesicle assembly promoted by α-synuclein. *Nature communications* **2016**, *7*, 1–12.

[52] Wennmalm, S.; Thyberg, P.; Xu, L.; Widengren, J. Inverse-fluorescence correlation spectroscopy. *Analytical chemistry* **2009**, *81*, 9209–9215.

[53] Braun, A. R.; Sevcsik, E.; Chin, P.; Rhoades, E.; Tristram-Nagle, S.; Sachs, J. N. α-Synuclein induces both positive mean curvature and negative Gaussian curvature in membranes. *Journal of the American Chemical Society* **2012**, *134*, 2613–2620.

[54] Corey, R. A.; Stansfeld, P. J.; Sansom, M. S. The energetics of protein–lipid interactions as viewed by molecular simulations. *Biochemical Society Transactions* **2020**, *48*, 25–37.

[55] Reynwar, B. J.; Illya, G.; Harmandaris, V. A.; Müller, M. M.; Kremer, K.; Deserno, M. Aggregation and vesiculation of membrane proteins by curvature-mediated interactions. *Nature* **2007**, *447*, 461–464.

[56] Spillantini, M. G.; Schmidt, M. L.; Lee, V. M.-Y.; Trojanowski, J. Q.; Jakes, R.; Goedert, M. α-Synuclein in Lewy bodies. *Nature* **1997**, *388*, 839–840.

[57] Shahmoradian, S. H.; Lewis, A. J.; Genoud, C.; Hench, J.; Moors, T. E.; Navarro, P. P.; Castaño-Díez, D.; Schweighauser, G.; Graff-Meyer, A.; Goldie, K. N., et al. Lewy pathology in Parkinson's disease consists of crowded organelles and lipid membranes. *Nature neuroscience* **2019**, *22*, 1099–1109.

[58] Galvagnion, C.; Buell, A. K.; Meisl, G.; Michaels, T. C.; Vendruscolo, M.; Knowles, T. P.; Dobson, C. M. Lipid vesicles trigger α-synuclein aggregation by stimulating primary nucleation. *Nature chemical biology* **2015**, *11*, 229–234.

[59] Gaspar, R.; Lund, M.; Sparr, E.; Linse, S. Anomalous Salt Dependence Reveals an Interplay of Attractive and Repulsive Electrostatic Interactions in α-synuclein Fibril Formation. *QRB Discovery* **2020**, *1*.

[60] Galvagnion, C.; Topgaard, D.; Makasewicz, K.; Buell, A. K.; Linse, S.; Sparr, E.; Dobson, C. M. Lipid dynamics and phase transition within α-synuclein amyloid fibrils. *The journal of physical chemistry letters* **2019**, *10*, 7872–7877.

Scientific Publications

Printed by Media-Tryck, Lund 2022 NORDIC SWAN ECOLABEL 3041 0903

LUND UNIVERSITY

ISBN: 978-91-7422-870-0

Physical Chemistry
Faculty of Science
Lund University